

# Searching for gluon saturation effects in momentum transfer dependence of coherent charmonium electroproduction off nuclei

J. Nemchik<sup>1,2\*</sup> and J. Óbertová<sup>1†</sup>

<sup>1</sup> *Czech Technical University in Prague, FNSPE, Břehová 7, 11519 Prague, Czech Republic and*

<sup>2</sup> *Institute of Experimental Physics SAS, Watsonova 47, 04001 Košice, Slovakia*

(Dated: July 3, 2025)

We study for the first time the transverse momentum transfer distributions  $d\sigma/dt$  in coherent production of charmonia in nuclear ultra-peripheral and electron-ion collisions within the QCD color dipole approach based on a rigorous Green function formalism. This allows us to treat properly the color transparency effects, as well as the higher and leading-twist shadowing corrections associated with the  $|Q\bar{Q}\rangle$  and  $|Q\bar{Q}nG\rangle$  Fock components of the photon. While the multi-gluon photon fluctuations represent the dominant source of nuclear shadowing at kinematic regions related to the recent LHC and its future upgrade to LHeC, the upcoming electron-ion collider at RHIC will additionally require the proper incorporation of reduced quark shadowing. The latter effect leads to a significant decrease in the differential cross sections  $d\sigma/dt$  compared to standard calculations based on the eikonal form for the dipole-nucleus amplitude. The leading-twist shadowing corrections, corresponding to a non-linear QCD evolution of a partial dipole-nucleus amplitude, reduce substantially charmonium  $t$ -distributions in the LHeC energy range. We predict a non-monotonic energy dependence of  $d\sigma/dt$  suggesting so possible gluon saturation effects with increased onset at larger  $t$ -values. In addition to shadowing corrections, we study how the color transparency effects affect the shape of  $t$ -dependent nuclear modification factor. We also briefly discuss several aspects that can modify the charmonium production rate and thus may have a large impact on the search for gluon saturation effects.

PACS numbers: 14.40.Pq, 13.60.Le, 13.60.-r

## I. INTRODUCTION

Recent experiments with ultra-peripheral collisions (UPC) at Relativistic Heavy Ion Collider (RHIC) and the Large Hadron Collider (LHC) (see e.g., [1]) offer new possibilities for investigation of exclusive photoproduction of vector mesons on protons and nuclei. [2]. Whereas the LHC kinematic region allows to study the space-time pattern of the diffraction mechanism [3] in coherent photoproduction of heavy quarkonia at high photon energies, the experiments on the planned Large Hadron-Electron Collider (LHeC) from the High Luminosity-LHC [4] will extend such studies also to an electroproduction process with a non-zero photon virtuality  $Q^2$ . Here the theoretical description is simplified due to the long coherence length (CL)  $l_c$  for the  $Q\bar{Q}$  photon fluctuation, much longer than the nuclear radius  $R_A$ ,

$$l_c = \frac{W^2 + Q^2 - m_N^2}{m_N(M_V^2 + Q^2)} \gg R_A, \quad (1.1)$$

where  $W$  is the c.m. energy of the photon-nucleon system;  $m_N$  and  $M_V$  are the masses of the nucleon and vector meson, respectively. The inequality (1.1) is related to the strongest onset of the initial state quark shadowing. Then the corresponding expressions for the nuclear cross sections lie on the eikonal form for the  $Q\bar{Q}$  dipole-nucleus cross section and/or for the impact-parameter-dependent partial amplitude [5–7]. The eikonal form is frequently adopted in the literature also in kinematic regions where the condition (1.1) is not completely fulfilled (see e.g., Ref. [8]).

Future experiments at the Electron-Ion Collider (EIC) [9–11] using the present RHIC facility will provide an opportunity to look inside a diffraction mechanism also in the kinematic region where  $l_c \lesssim R_A$ . Here, one cannot use the eikonal approximation anymore and more sophisticated formalism is required to describe quantum coherence

---

\*Electronic address: jan.nemcik@fjfi.cvut.cz

†Electronic address: jarooslava.obertova@fjfi.cvut.cz

(QC) effects. In heavy quarkonium electroproduction, a short lifetime of the  $Q\bar{Q}$  photon fluctuation,  $l_c \ll R_A$ , is correlated with a much longer formation time (length) (FL) [12],  $t_f \sim R_A$ , controlling the evolution of the  $Q\bar{Q}$  wave packet during propagation through the medium. The magnitude of  $t_f$  can be obtained in the rest frame of the nucleus from the uncertainty principle,

$$t_f = \frac{W^2 + Q^2 - m_N^2}{m_N(M_{V'}^2 - M_V^2)} \approx l_c \cdot \frac{M_V^2 + Q^2}{M_{V'}^2 - M_V^2} = l_c \cdot \left[ \frac{M_{V'}^2 + Q^2}{M_{V'}^2 - M_V^2} - 1 \right], \quad (1.2)$$

where  $M_{V'}$  is the mass of radially excited quarkonium. The propagation of the  $Q\bar{Q}$  pair in the medium is related to the color transparency (CT) effect (see e.g., Refs. [13–16]), which represents the final state absorption of the produced quarkonia. Here the medium becomes more transparent for  $Q\bar{Q}$  dipole configurations with smaller transverse sizes. Note that in the electroproduction of heavy quarkonia there is a strong inequality,  $l_c \ll l_f$ , as follows from Eq. (1.2).

The description of the diffraction mechanism in terms of color dipoles has a long-standing history starting from Ref. [13] and has been applied to exclusive photo- and electroproduction of heavy quarkonia on protons and nuclei (see e.g., Refs. [14, 17–20]). In our recent work [21] we have studied the coherent process  $\gamma^*A \rightarrow VA$  ( $V = J/\Psi(1S), \psi'(2S)$ ) including properly the above mentioned effects of QC and CT within a rigorous quantum mechanical approach based on the Green function formalism. We have performed corresponding predictions for  $t$ -integrated<sup>1</sup> production cross sections that can be verified by future experiments at the EIC.

In Ref. [6], the  $t$ -dependent differential cross sections  $d\sigma^{\gamma^*A \rightarrow VA}/dt$  have been studied in the LHC kinematic region of recent experiments with UPC, where the eikonal approximation related to the condition (1.1) can be safely adopted. In the present work, we improve such predictions extending them also to the kinematic region beyond the validity of Eq. (1.1). This requires to incorporate the reduced effects of QC by applying the path integral technique. Simultaneously we aim to minimize all known theoretical uncertainties of the quantum chromodynamics (QCD) dipole formalism, related to quarkonium S-wave functions together with elimination of D-wave component, dipole orientation, as well as the magnitude of the leading-twist shadowing corrections. Consequently, this may lead to increased efficiency in searching for a conclusive signal of gluon saturation effects [22].

We include the correlation between the dipole transverse orientation  $\vec{r}$  and the impact parameter of the collision  $\vec{b}$  [23]. This effect causes that the  $Q\bar{Q}$  dipole-nucleon interaction vanishes when  $\vec{r} \perp \vec{b}$  but reaches maximal strength when  $\vec{r} \parallel \vec{b}$ . However, it is missed in many calculations. The  $\vec{r}$ - $\vec{b}$  correlation has been treated in Ref. [24], but not properly incorporated, since the  $\vec{b}$ -dependent dipole-nucleon amplitude  $\mathcal{A}_{Q\bar{Q}}^N(\vec{r}, \vec{b})$  after integration over  $\vec{b}$  exhibits a non-monotonic behavior as a function of the dipole size  $r$ . Besides, this amplitude  $\mathcal{A}_{Q\bar{Q}}^N(\vec{r}, \vec{b})$  leads to incorrect limiting values when  $b \rightarrow 0$  and  $b \sim R_A$  (see a brief discussion in point iii) of Sec. IV E).

The impact of the  $\vec{r}$ - $\vec{b}$  correlation on the magnitude of differential cross sections in exclusive photo-production of heavy quarkonia on protons has been studied in Ref. [20]. The nodal structure of the wave functions for radially excited heavy quarkonium states enhances the onset of the correlation effect and thus provides additional constraints on the models for the  $b$ -dependent dipole amplitude. The importance of the color dipole orientation in other processes has been discussed in Ref. [20] (see also references therein). The  $\vec{r}$ - $\vec{b}$  correlation has been also omitted in Ref. [25] analyzing the impact-parameter dependence in the initial condition of the Balitsky–Kovchegov (BK) equation [26, 27].

We expect a rather small effect of the  $\vec{r}$ - $\vec{b}$  correlation in processes on nuclear targets [6]. A rather weak impact of the dipole orientation on the azimuthal asymmetry of photons and pions has been found and analyzed in Refs. [23, 28–30]. Nevertheless, in the present paper, we implement this effect in calculations of  $d\sigma^{\gamma^*A \rightarrow VA}/dt$ , thus minimizing the theoretical uncertainties. On the other hand, the  $\vec{r}$ - $\vec{b}$  correlation has a large impact on the magnitudes of  $t$ -dependent nuclear transparency, Eq. (4.2), which is effective for the study of CT effects.

The LHC and LHeC kinematic region, related to the condition (1.1), gives rise to a maximal strength of the higher-twist quark shadowing. However, such a shadowing correction is rather small for the photo- and electroproduction of heavy quarkonia due to the large heavy quark mass. Then the main nuclear effect comes from the leading-twist gluon shadowing, which is related to the higher Fock components of the projectile photon containing gluons. According to the analysis in Ref. [6], the dominant contribution to nuclear shadowing comes from the  $|Q\bar{Q}G\rangle$  Fock component. We implement the gluon shadowing (GS) corrections in our calculations of nuclear cross sections from Refs. [6, 18, 31]. Inclusion of higher multi-gluon Fock components  $|Q\bar{Q}nG\rangle$  is still a challenge. However, their effect is essentially taken into account by the eikonalization of the GS correction factor.

The LHeC kinematic region allows to analyze how a modification of the gluon distribution in nuclei by the GS corrections affects the  $t$ -dependent differential cross sections. In the infinite momentum frame, the phenomenon of

<sup>1</sup>  $t = -q^2$ , where  $\vec{q}$  is the transverse component of the momentum transfer.

GS looks similar to gluon-gluon fusion corresponding to a non-linear term in evolution equations [26, 27, 32, 33]. We expect a suppression of small- $x$  gluons and a precocious onset of saturation effects, especially for heavy nuclei. This may lead to a non-monotonic energy dependence of  $d\sigma^{\gamma^*A \rightarrow VA}/dt$  at fixed  $t$ -values. Such an expectation is explored in the present work and represents one of the main goals of our study. Note that a non-monotonic energy dependence of  $d\sigma/dt$  has been presented at large  $t \sim 1 \text{ GeV}^2$  also in Ref. [34] studying the incoherent production of  $J/\psi$  on the lead target within the hot-spot model. However, the important effect of gluon shadowing has been ignored. This may have a large impact on the reliability of the predicted onset of saturation effects.

The present paper is organized as follows. In the next Sec. II we briefly present the dipole formalism for electroproduction on a proton target,  $\gamma^*p \rightarrow Vp$ , in terms of the  $\vec{b}$ -dependent dipole amplitude. The Sec. III is devoted to the coherent heavy quarkonium production on nuclear targets,  $\gamma^*A \rightarrow VA$ . Here we present expressions for the  $t$ -dependent differential cross sections  $d\sigma^{\gamma^*A \rightarrow VA}/dt$  within a rigorous Green function formalism. Consequently, in Sec. IV A we first compare our model calculations of  $d\sigma^{\gamma^*p \rightarrow Vp}/dt$  ( $V = J/\psi(1S)$  and  $\psi'(2S)$ ) and  $\sigma^{\gamma p \rightarrow \psi'(2S)p}$  with available data from experiments at the Hadron–Electron Ring Accelerator (HERA) and the LHC. Then in Sec. IV B we propose how manifestations of CT effects may be recognized by the future EIC measurements. Sec. IV C is devoted to predictions for  $d\sigma/dt$  in the coherent photo- and electroproduction of 1S and 2S charmonium states off nuclei in kinematic regions accessible by upcoming EIC experiments at RHIC and the LHeC. Here we analyze the impact of reduced quantum coherence effects for  $Q\bar{Q}$  photon fluctuations on magnitudes of the  $t$ -dependent nuclear differential cross sections at small photon energies  $W$ , when  $l_c \lesssim R_A$ , for fixed values of  $Q^2$  and  $t$ . Moreover, for the LHeC kinematic region, we predict in Sec. IV D the possible onset of saturation effects, manifested via a non-monotonic energy behavior of  $d\sigma^{\gamma^*A \rightarrow VA}/dt$ . Finally, in Sec. IV E we briefly mention and discuss possible pitfalls in searching for gluon saturation effects. The last Sec. V contains summary and discussion of our results.

## II. ELECTRO-PRODUCTION OF HEAVY QUARKONIA ON PROTONS

Within the light-front (LF) color dipole formalism, the amplitude for the electroproduction of heavy quarkonia with the transverse component of momentum transfer  $\vec{q}$  takes the following factorized form [14],

$$\mathcal{A}^{\gamma^*p \rightarrow Vp}(x, Q^2, \vec{q}) = \langle V | \tilde{\mathcal{A}} | \gamma^* \rangle = \int d^2r \int_0^1 d\alpha \Psi_V^*(\vec{r}, \alpha) \mathcal{A}_{Q\bar{Q}}(\vec{r}, x, \alpha, \vec{q}) \Psi_{\gamma^*}(\vec{r}, \alpha, Q^2). \quad (2.1)$$

Here  $\mathcal{A}_{Q\bar{Q}}(\vec{r}, x, \alpha, \vec{q})$  is the amplitude for the elastic scattering of the color dipole on a nucleon target.

It is convenient to study differential cross sections  $d\sigma/dq^2$  treating the partial dipole scattering amplitude in the impact parameter representation  $\mathcal{A}_{Q\bar{Q}}(\vec{r}, x, \alpha, \vec{b})$  related to the  $\vec{q}$ -dependent amplitude by Fourier transform,

$$\mathcal{A}_{Q\bar{Q}}(\vec{r}, x, \alpha, \vec{q}) = \int d^2b e^{i\vec{b}\cdot\vec{q}} \mathcal{A}_{Q\bar{Q}}(\vec{r}, x, \alpha, \vec{b}), \quad (2.2)$$

which correctly reproduces the dipole cross section at  $\vec{q} = 0$ ,

$$\sigma_{Q\bar{Q}}(r, x) = \text{Im} \mathcal{A}_{Q\bar{Q}}(\vec{r}, x, \alpha, \vec{q} = 0) = 2 \int d^2b \text{Im} \mathcal{A}_{Q\bar{Q}}^N(\vec{r}, x, \alpha, \vec{b}). \quad (2.3)$$

In Eq. (2.1), the variable  $\Psi_V(r, \alpha)$  is the LF wave function for heavy quarkonium and  $\Psi_{\gamma^*}(r, \alpha, Q^2)$  is the LF distribution of the  $Q\bar{Q}$  Fock component of the real ( $Q^2 = 0$ ) or virtual ( $Q^2 > 0$ ) photon, with transverse separation  $\vec{r}$ . The variable  $\alpha$  is the fractional LF momentum carried by a heavy quark or antiquark from a  $Q\bar{Q}$  Fock component of the photon.

Combining Eqs. (2.1)-(2.3) the electroproduction amplitude  $\mathcal{A}^{\gamma^*p \rightarrow Vp}(x, Q^2, \vec{q})$  has the following form,

$$\mathcal{A}^{\gamma^*p \rightarrow Vp}(x, Q^2, \vec{q}) = 2 \int d^2b e^{i\vec{b}\cdot\vec{q}} \int d^2r \int_0^1 d\alpha e^{i(1/2-\alpha)\vec{r}\cdot\vec{q}} \Psi_V^*(\vec{r}, \alpha) \text{Im} \mathcal{A}_{Q\bar{Q}}^N(\vec{r}, x, \alpha, \vec{b}) \Psi_{\gamma^*}(\vec{r}, \alpha, Q^2), \quad (2.4)$$

where the argument in the  $\alpha$ -dependent phase factor includes the fact that the relative distance of  $Q$  or  $\bar{Q}$  from the  $Q\bar{Q}$  center of gravity varies with the fractional LF momenta as  $r\alpha$  or  $r(1-\alpha)$ .

The amplitude (2.4) depends on Bjorken  $x$  evaluated in [35] in the leading  $\log(1/x)$  approximation,

$$x = \frac{M_V^2 + Q^2}{s} = \frac{M_V^2 + Q^2}{W^2 + Q^2 - m_N^2}. \quad (2.5)$$

The essential feature of the dipole-proton partial amplitude  $\mathcal{A}_{Q\bar{Q}}^N(\vec{r}, x, \alpha, \vec{b})$  in Eq. (2.4) is the  $\vec{r}\text{-}\vec{b}$  correlation. Its explicit form was proposed in Refs. [20, 23, 28–30] and is as follows,

$$\text{Im}\mathcal{A}_{Q\bar{Q}}^N(\vec{r}, x, \alpha, \vec{b}) = \frac{\sigma_0}{8\pi\mathcal{B}(x)} \left\{ \exp\left[-\frac{[\vec{b} + \vec{r}(1-\alpha)]^2}{2\mathcal{B}(x)}\right] + \exp\left[-\frac{(\vec{b} - \vec{r}\alpha)^2}{2\mathcal{B}(x)}\right] - 2 \exp\left[-\frac{r^2}{R_0^2(x)} - \frac{[\vec{b} + (1/2 - \alpha)\vec{r}]^2}{2\mathcal{B}(x)}\right] \right\}, \quad (2.6)$$

where the function  $\mathcal{B}(x)$  was defined in Ref. [30] as,

$$\mathcal{B}(x) = B_{el}^{\bar{q}q}(x, r \rightarrow 0) - \frac{1}{8}R_0^2(x). \quad (2.7)$$

Here  $R_0^2(x)$  controls the  $x$  dependence of the saturation cross section, introduced in [36, 37],  $\sigma_{Q\bar{Q}}(r, x) = \sigma_0 (1 - \exp[-r^2/R_0^2(x)])$ . We adopt parameters from the recent work [38],  $\sigma_0 = 25.21$  mb,  $R_0(x) = 0.4$  fm  $\times (x/x_0)^{0.1405}$  with  $x_0 = 0.80 \times 10^{-4}$ , referred to as the GBS-0 model.

The dipole-proton slope in the limit of vanishingly small dipoles  $B_{el}^{\bar{q}q}(x, r \rightarrow 0)$  can be measured in the electroproduction of vector mesons with highly virtual photons  $Q^2 \gg 1$  GeV<sup>2</sup>. The measured slope  $B_{\gamma^*p \rightarrow \rho p}(x, Q^2 \gg 1$  GeV<sup>2</sup>)  $\approx 5$  GeV<sup>-2</sup> [39] is, as expected [40], defined by the proton charge radius.

The GBS-0 model mentioned above lacks the Dokshitzer-Gribov-Lipatov-Altarelli-Parisi (DGLAP) evolution. However, Ref. [38] also contains the same model with such an evolution. Here the saturation scale is related to the gluon density, which is subject to the DGLAP evolution,  $R_0^2(x, \mu^2) = 4/Q_s^2(x, \mu^2) = \sigma_0 N_c / (\pi^2 \alpha_s(\mu^2) x g(x, \mu^2))$ , where  $\mu^2 = C/r^2 + \mu_0^2$ ,  $Q_s^2$  is the saturation scale, and the gluon distribution function  $x g(x, \mu^2)$  is obtained as a solution of the DGLAP evolution equation with the form at the initial scale  $Q_0^2 = 1$  GeV<sup>2</sup>,  $x g(x, Q_0^2) = A_g x^{-\lambda_g} (1-x)^{5.6}$ . Here  $A_g = 1.07$ ,  $\lambda_g = 0.11$ ,  $\mu_0^2 = 1.74$  GeV<sup>2</sup>,  $C = 0.27$  and  $\sigma_0 = 22.93$  mb. In what follows, we will refer to the GBS dipole model as to the GBS-0 model containing the DGLAP evolution and the color dipole orientation (2.6).

Treating the electroproduction of heavy quarkonia and assuming the  $s$ -channel helicity conservation, the  $t$ -dependent differential cross section can be expressed as a sum of  $T$  and  $L$  contributions for transversely and longitudinally polarized photons and vector mesons, respectively,

$$\begin{aligned} \frac{d\sigma^{\gamma^*p \rightarrow Vp}(x, Q^2, t = -q^2)}{dt} &= \frac{d\sigma_T^{\gamma^*p \rightarrow Vp}(x, Q^2, t)}{dt} + \tilde{\varepsilon} \frac{d\sigma_L^{\gamma^*p \rightarrow Vp}(x, Q^2, t)}{dt} \\ &= \frac{1}{16\pi} \left( \left| \mathcal{A}_T^{\gamma^*p \rightarrow Vp}(x, Q^2, \vec{q}) \right|^2 + \tilde{\varepsilon} \left| \mathcal{A}_L^{\gamma^*p \rightarrow Vp}(x, Q^2, \vec{q}) \right|^2 \right), \end{aligned} \quad (2.8)$$

where we have taken the photon polarization  $\tilde{\varepsilon} = 0.99$ .

We also include a small real part [41–43] of the  $\gamma^*p \rightarrow Vp$  amplitude performing the following replacement in Eq. (2.4),

$$\text{Im}\mathcal{A}_{Q\bar{Q}}^N(\vec{r}, x, \alpha, \vec{b}) \Rightarrow \text{Im}\mathcal{A}_{Q\bar{Q}}^N(\vec{r}, x, \alpha, \vec{b}) \cdot \left(1 - i \frac{\pi\Lambda}{2}\right), \quad \Lambda = \frac{\partial \ln(\text{Im}\mathcal{A}_{Q\bar{Q}}^N(\vec{r}, x, \alpha, \vec{b}))}{\partial \ln(1/x)}. \quad (2.9)$$

In order to include the skewness correction [44] we perform the following modification,

$$\text{Im}\mathcal{A}_{Q\bar{Q}}^N(\vec{r}, x, \alpha, \vec{b}) \Rightarrow \text{Im}\mathcal{A}_{Q\bar{Q}}^N(\vec{r}, x, \alpha, \vec{b}) \cdot R_S(\Lambda) \quad (2.10)$$

where the skewness factor  $R_S(\Lambda) = (2^{2\Lambda+3}/\sqrt{\pi}) \cdot \Gamma(\Lambda + 5/2)/\Gamma(\Lambda + 4)$ .

In our previous works [5, 19–21, 45–47] (see also Sec. II.A in Ref. [6]) we ruled out the possibility of a photon-like vertex for the transition of a heavy quarkonium to a  $Q\bar{Q}$  pair due to the unusually large weight of a  $D$ -wave component in the rest frame wave function, in contrast to solutions of the Schrödinger equation. Instead, we rely on the quarkonium LF wave functions obtained from a solution of the Lorentz boosted Schrödinger equation [48] with realistic potentials. Although several such potentials can be found in the literature, in the present paper we choose only the power-like potential (POW) [49]. This potential in combination with the GBS model [38] for the dipole cross section provides the best description of the UPC data, as shown in Ref. [21]. Since the quark transverse momenta are not parallel to the boost axis, a significant correction to the boosting prescription [50] from the rest frame to the

LF frame is taken into account, known as the Melosh spin rotation [51] (see also [19, 52]). This leads to the following specific form of the electroproduction amplitudes given by Eq. (2.4) for  $T$  and  $L$  polarizations,

$$\begin{aligned} \mathcal{A}_T^{\gamma^* p \rightarrow V p}(x, Q^2, \vec{q}) &= N_p \int d^2 r \int_0^1 d\alpha \int d^2 b \exp\left[i[\vec{b} + (1/2 - \alpha)\vec{r}] \cdot \vec{q}\right] \\ &\quad \times \text{Im} \mathcal{A}_{Q\bar{Q}}^N(\vec{r}, x, \alpha, \vec{b}) \left[ \Sigma_T^{(1)}(r, \alpha, Q^2) + \Sigma_T^{(2)}(r, \alpha, Q^2) \right], \\ \Sigma_T^{(1)}(r, \alpha, Q^2) &= K_0(\eta r) \int_0^\infty dp_T p_T J_0(p_T r) \Psi_V(\alpha, p_T) \left[ \frac{2m_Q^2(m_L + m_T) + m_L p_T^2}{m_T(m_L + m_T)} \right], \\ \Sigma_T^{(2)}(r, \alpha, Q^2) &= K_1(\eta r) \int_0^\infty dp_T p_T^2 J_1(p_T r) \Psi_V(\alpha, p_T) \left[ \eta \frac{m_Q^2(m_L + 2m_T) - m_T m_L^2}{m_Q^2 m_T(m_L + m_T)} \right], \end{aligned} \quad (2.11)$$

and

$$\begin{aligned} \mathcal{A}_L^{\gamma^* p \rightarrow V p}(x, Q^2, \vec{q}) &= N_p \int d^2 r \int_0^1 d\alpha \int d^2 b \exp\left[i[\vec{b} + (1/2 - \alpha)\vec{r}] \cdot \vec{q}\right] \text{Im} \mathcal{A}_{Q\bar{Q}}^N(\vec{r}, x, \alpha, \vec{b}) \Sigma_L(r, \alpha, Q^2), \\ \Sigma_L(r, \alpha, Q^2) &= K_0(\eta r) \int_0^\infty dp_T p_T J_0(p_T r) \Psi_V(\alpha, p_T) \left[ 4Q\alpha(1 - \alpha) \frac{m_Q^2 + m_L m_T}{m_Q(m_L + m_T)} \right], \end{aligned} \quad (2.12)$$

where  $N_p = Z_Q \sqrt{2N_c \alpha_{em}} / 2\pi$ ;  $\eta^2 = m_Q^2 + \alpha(1 - \alpha)Q^2$ ;  $m_Q$  is the heavy quark mass;  $\alpha_{em} = 1/137$  is the fine-structure constant; the factor  $N_c = 3$  represents the number of colors in QCD;  $Z_Q = 2/3$  is the charge isospin factor for charmonium production; variables  $m_T = \sqrt{m_Q^2 + p_T^2}$  and  $m_L = 2m_Q \sqrt{\alpha(1 - \alpha)}$ , and  $J_{0,1}$  and  $K_{0,1}$  are the Bessel functions of the first kind and the modified Bessel functions of the second kind, respectively.

### III. COHERENT ELECTROPRODUCTION OFF NUCLEI: MOMENTUM TRANSFER DEPENDENCE IN THE GREEN FUNCTION FORMALISM

In this Section we focus on the lowest  $|Q\bar{Q}\rangle$  Fock component of the projectile photon. Since the  $Q\bar{Q}$  transverse size is small,  $\propto 1/\eta$ , the shadowing corrections are as small as  $1/\eta^2$ , so they should be treated as a higher-twist effect. Within the Green function formalism, the amplitude for quarkonium electroproduction on a nuclear target,  $\gamma^* A \rightarrow VA$ , is given by the following expression,

$$\mathcal{A}^{\gamma^* A \rightarrow VA}(x, Q^2, \vec{q}) = 2 \int d^2 b \int d^2 b_A \exp\left[i(\vec{b} + \vec{b}_A) \cdot \vec{q}\right] \int_{-\infty}^\infty dz \rho_A(\vec{b} + \vec{b}_A, z) F_1(x, \vec{b}, \vec{b}_A, z), \quad (3.1)$$

where  $\rho_A(b, z)$  is the nuclear density distribution, for which we employ the realistic Wood-Saxon form with parameters taken from Ref. [53];  $\vec{b}_A$  is the nuclear impact parameter and the function  $F_1(x, \vec{b}, \vec{b}_A, z)$  can be expressed as,

$$\begin{aligned} F_1(x, \vec{b}, \vec{b}_A, z) &= \int_0^1 d\alpha \int d^2 r_1 d^2 r_2 \Psi_V^*(\vec{r}_2, \alpha) G_{Q\bar{Q}}(z' \rightarrow \infty, \vec{r}_2; z, \vec{r}_1 | \vec{b}_A) \\ &\quad \times \exp\left[i(1/2 - \alpha)\vec{r}_1 \cdot \vec{q}\right] \mathcal{A}_{Q\bar{Q}}^N(\vec{r}_1, x, \alpha, \vec{b}) \Psi_{\gamma^*}(\vec{r}_1, \alpha, Q^2). \end{aligned} \quad (3.2)$$

Here the function  $F_1(x, \vec{b}, \vec{b}_A, z)$  describes the coherent (elastic) production of the colorless  $Q\bar{Q}$  pair of initial separation  $\vec{r}_1$  at point  $z$  with its subsequent evolution during propagation through the nucleus which is completed by the formation of the heavy quarkonium wave function at  $z' \rightarrow \infty$  with final separation  $\vec{r}_2$ . Such an evolution of an interacting  $Q\bar{Q}$  pair is described by the corresponding Green function  $G_{Q\bar{Q}}(z', \vec{r}_2; z, \vec{r}_1 | \vec{b}_A)$ , which satisfies the two-dimensional Schrödinger equation [12, 31]

$$i \frac{d}{dz_2} G_{Q\bar{Q}}(z_2, \vec{r}_2; z_1, \vec{r}_1 | \vec{b}_A) = \left[ \frac{\eta^2 - \Delta_{r_2}}{2p\alpha(1 - \alpha)} + V_{Q\bar{Q}}(z_2, \vec{r}_2, \alpha, \vec{b}_A) \right] G_{Q\bar{Q}}(z_2, \vec{r}_2; z_1, \vec{r}_1 | \vec{b}_A), \quad (3.3)$$

where  $p$  is the photon energy in the target rest frame and the Laplacian  $\Delta_{r_2}$  acts on the coordinate  $r_2$ .

The real part of the LF potential  $V_{Q\bar{Q}}(z_2, \vec{r}_2, \alpha)$  in Eq. (3.3) describes the interaction between the  $Q$  and  $\bar{Q}$ . In Ref. [21] we have proposed a procedure how to obtain  $\text{Re}V_{Q\bar{Q}}(z_2, \vec{r}_2, \alpha)$  in the LF frame from various realistic  $Q\bar{Q}$

interaction models defined in the rest frame. Such potentials lead to a correct shape of quarkonium wave functions in the LF frame. As in the case of the nucleon target, for the coherent process  $\gamma^*A \rightarrow VA$  we also adopt the POW model [49] for the realistic interaction potential in the  $Q\bar{Q}$  rest frame.

The imaginary part of the the LF potential  $V_{Q\bar{Q}}(z_2, \vec{r}_2, \alpha)$  in Eq. (3.3) controls the attenuation of the  $|Q\bar{Q}\rangle$  Fock state of the photon in the medium. It has the following form,

$$\text{Im}V_{Q\bar{Q}}(z_2, \vec{r}, \alpha, \vec{b}_A) = - \int d^2b' \mathcal{A}_{Q\bar{Q}}^N(\vec{r}, x, \alpha, \vec{b}') \rho_A(\vec{b}' + \vec{b}_A, z_2). \quad (3.4)$$

The final form of the nuclear  $t$ -dependent production amplitudes for both the T and L polarizations, including the spin rotation effects, has a structure that is more complicated compared to the proton target, Eqs. (2.11) and (2.12), and reads,

$$\begin{aligned} \mathcal{A}_T^{\gamma^*A \rightarrow VA}(x, Q^2, \vec{q}) &= 2N_p \int d^2b \int d^2b_A \exp\left[i(\vec{b} + \vec{b}_A) \cdot \vec{q}\right] \int_{-\infty}^{\infty} dz \rho_A(\vec{b} + \vec{b}_A, z) \\ &\times \int d^2r_1 \int d^2r_2 \int_0^1 d\alpha \exp\left[i(1/2 - \alpha) \vec{r}_1 \cdot \vec{q}\right] \\ &\times \mathcal{A}_{Q\bar{Q}}^N(\vec{r}_1, x, \alpha, \vec{b}) G_{Q\bar{Q}}(z' \rightarrow \infty, \vec{r}_2; z, \vec{r}_1 | \vec{b}_A) \left[ \Gamma_T^{(1)}(r_1, r_2, \alpha, Q^2) + \Gamma_T^{(2)}(r_1, r_2, \alpha, Q^2) \right], \\ \Gamma_T^{(1)}(r_1, r_2, \alpha, Q^2) &= K_0(\eta r_1) \int_0^{\infty} dp_T p_T J_0(p_T r_2) \Psi_V(\alpha, p_T) \left[ \frac{2m_Q^2(m_L + m_T) + m_L p_T^2}{m_T(m_L + m_T)} \right], \\ \Gamma_T^{(2)}(r_1, r_2, \alpha, Q^2) &= K_1(\eta r_1) \int_0^{\infty} dp_T p_T^2 J_1(p_T r_2) \Psi_V(\alpha, p_T) \left[ \eta \frac{m_Q^2(m_L + 2m_T) - m_T m_L^2}{m_Q^2 m_T(m_L + m_T)} \right], \end{aligned} \quad (3.5)$$

and

$$\begin{aligned} \mathcal{A}_L^{\gamma^*A \rightarrow VA}(x, Q^2, \vec{q}) &= 2N_p \int d^2b \int d^2b_A \exp\left[i(\vec{b} + \vec{b}_A) \cdot \vec{q}\right] \int_{-\infty}^{\infty} dz \rho_A(\vec{b} + \vec{b}_A, z) \\ &\times \int d^2r_1 \int d^2r_2 \int_0^1 d\alpha \exp\left[i(1/2 - \alpha) \vec{r}_1 \cdot \vec{q}\right] \\ &\times \mathcal{A}_{Q\bar{Q}}^N(\vec{r}_1, x, \alpha, \vec{b}) G_{Q\bar{Q}}(z' \rightarrow \infty, \vec{r}_2; z, \vec{r}_1 | \vec{b}_A) \Gamma_L(r_1, r_2, \alpha, Q^2), \\ \Gamma_L(r_1, r_2, \alpha, Q^2) &= K_0(\eta r_1) \int_0^{\infty} dp_T p_T J_0(p_T r_2) \Psi_V(\alpha, p_T) \left[ 4Q\alpha(1 - \alpha) \frac{m_Q^2 + m_L m_T}{m_Q(m_L + m_T)} \right]. \end{aligned} \quad (3.6)$$

The expression for the  $t$ -dependent differential cross section reads

$$\frac{d\sigma^{\gamma^*A \rightarrow VA}(x, Q^2, t = -q^2)}{dt} = \frac{1}{16\pi} \left( \left| \mathcal{A}_T^{\gamma^*A \rightarrow VA}(x, Q^2, \vec{q}) \right|^2 + \varepsilon \left| \mathcal{A}_L^{\gamma^*A \rightarrow VA}(x, Q^2, \vec{q}) \right|^2 \right). \quad (3.7)$$

Note that the Green function formalism can be applied to coherent processes without any restrictions for the coherence length  $l_c$ , for arbitrary realistic  $Q\bar{Q}$  interaction potential, as well as for any phenomenological model for the impact parameter-dependent partial dipole amplitude.

At high photon energies, corresponding to  $x \lesssim 0.01$ , the condition (1.1) is valid and the so-called *long coherence length* (LCL) regime is at work. Then the eikonal approximation can be applied as a limiting case of the Green function formalism, when the Green function acquires a simple form,

$$G_{Q\bar{Q}}(z_2, \vec{r}_2; z_1, \vec{r}_1) \Rightarrow \delta^{(2)}(\vec{r}_1 - \vec{r}_2) \exp \left[ - \int d^2b \mathcal{A}_{Q\bar{Q}}^N(\vec{r}_1, x, \alpha, \vec{b}) \int_{z_1}^{z_2} dz \rho_A(\vec{b} + \vec{b}_A, z) \right], \quad (3.8)$$

and the Lorentz time dilation freezes the transverse sizes of such long-lived  $Q\bar{Q}$  photon fluctuations during propagation through the medium. Such an LCL effect is also known as the "frozen" approximation. Then the  $t$ -dependent amplitude of quarkonium electroproduction on a nuclear target,  $\gamma^*A \rightarrow VA$  is given by the expression (2.4), but replacing the dipole-nucleon by dipole-nucleus amplitude  $\mathcal{A}_{Q\bar{Q}}^N(\vec{r}, x, \alpha, \vec{b}) \Rightarrow \mathcal{A}_{Q\bar{Q}}^A(\vec{r}, x, \alpha, \vec{b}_A)$  and  $\vec{b} \Rightarrow \vec{b}_A$ ,

$$\mathcal{A}^{\gamma^*A \rightarrow VA}(x, Q^2, \vec{q}) = 2 \int d^2b_A e^{i\vec{q} \cdot \vec{b}_A} \int d^2r \int_0^1 d\alpha e^{i(1/2 - \alpha) \vec{r} \cdot \vec{q}} \cdot \Psi_V^*(\vec{r}, \alpha) \mathcal{A}_{Q\bar{Q}}^A(\vec{r}, x, \alpha, \vec{b}_A) \Psi_{\gamma^*}(\vec{r}, \alpha, Q^2), \quad (3.9)$$

where one can rely on the eikonal form for the dipole-nucleus partial amplitude at nuclear impact parameter  $\vec{b}_A$ ,

$$\begin{aligned} \text{Im}\mathcal{A}_{\bar{Q}Q}^A(\vec{r}, x, \alpha, \vec{b}_A) \Big|_{l_c \gg R_A} &= 1 - \left[ 1 - \frac{1}{A} \int d^2b \text{Im}\mathcal{A}_{\bar{Q}Q}^N(\vec{r}, x, \alpha, \vec{b}) T_A(\vec{b}_A + \vec{b}) \right]^A \\ &\approx 1 - \exp \left[ - \int d^2b \text{Im}\mathcal{A}_{\bar{Q}Q}^N(\vec{r}, x, \alpha, \vec{b}) T_A(\vec{b}_A + \vec{b}) \right]. \end{aligned} \quad (3.10)$$

Here  $T_A(\vec{b}_A) = \int_{-\infty}^{\infty} dz \rho_A(\vec{b}_A, z)$  is the nuclear thickness function normalized as  $\int d^2b_A T_A(\vec{b}_A) = A$ .

Similarly as for the proton target, the real part of the  $t$ -dependent nuclear  $\gamma^*A \rightarrow VA$  amplitude and the skewness correction are incorporated via substitutions (2.9) and (2.10) into Eqs. (3.4), (3.5) and (3.6).

Besides the effect of the reduced coherence length when  $l_c \lesssim (1 \div 2) \cdot R_A$ , the photoproduction of heavy quarkonia is also affected by the gluon shadowing as shown in Refs. [5, 6, 21, 54]. The leading-twist gluon shadowing was introduced in Ref. [31] within the dipole representation as a shadowing correction corresponding to higher Fock components of the photon containing gluons, i.e.,  $|Q\bar{Q}G\rangle$ ,  $|Q\bar{Q}2G\rangle$ , ... ,  $|Q\bar{Q}nG\rangle$ . However, in agreement with the analysis and discussion in Ref. [6], the high-energy part of the EIC kinematic region at RHIC and UPC kinematic region at the LHC generate a dominant contribution to the nuclear shadowing coming only from one-gluon Fock state  $|Q\bar{Q}G\rangle$  of the photon. The corresponding coherence (radiation) length has the form

$$l_c^G = \frac{(W^2 + Q^2 - m_N^2) \cdot \alpha_g(1 - \alpha_g)}{m_N \left[ k_T^2 + (1 - \alpha_g) m_g^2 + \alpha_g M_{\bar{Q}Q}^2 + \alpha_g(1 - \alpha_g) Q^2 \right]}, \quad (3.11)$$

where  $\alpha_g$  is the LF fraction of the photon momentum carried by the gluon,  $M_{\bar{Q}Q}$  is the effective mass of the  $\bar{Q}Q$  pair and the effective gluon mass  $m_g \approx 0.7 \text{ GeV}$  is fixed by data on gluon radiation [31, 55]. The condition for the onset of GS is a sufficiently long  $l_c^G \gg d$ , where  $d \approx 2 \text{ fm}$  is the mean separation between bound nucleons. One can also see that  $l_c^G \ll l_c$  due to small  $\alpha_g \ll 1$ , in agreement with calculations in Ref. [56]. We have incorporated the GS correction in our calculations as a reduction of the partial  $b$ -dependent dipole amplitude in nuclear reactions with respect to processes on nucleon [6, 57],

$$\text{Im}\mathcal{A}_{\bar{Q}Q}^N(\vec{r}, x, \alpha, \vec{b}) \Rightarrow \text{Im}\mathcal{A}_{\bar{Q}Q}^N(\vec{r}, x, \alpha, \vec{b}) \cdot R_G(x, |\vec{b}_A + \vec{b}|), \quad (3.12)$$

where the correction factor  $R_G(x, b)$ , related to the  $Q\bar{Q}G$  component of the photon, was calculated within the Green function formalism [12, 15, 18, 21, 31, 57–59] (see also Fig. 1 in Ref. [6]).

Note that the calculations of higher multi-gluon Fock components are very complex within the Green function formalism and represent thus a challenge. However, using renormalization (3.12), the corresponding shadowing corrections are included essentially via eikonalization of the factor  $R_G(x, b)$  (see discussion in Ref. [57]).

## IV. PREDICTIONS WITHIN THE GREEN FUNCTION FORMALISM

### A. Model calculations vs. data

In the present paper we apply the recent GBS model with DGLAP evolution [38] for the dipole-proton partial amplitude including correlation between the dipole transverse orientation  $\vec{r}$  and the impact parameter of the collision  $\vec{b}$ , Eq. (2.6). Our calculations rely on the quarkonium wave functions generated by the POW  $Q\bar{Q}$  interaction potential [49], since in combination with the GBS model provides the best description of the UPC data on rapidity distributions  $d\sigma/dy$  (see Ref. [21]). We also include the leading-twist gluon shadowing representing the main nuclear effect in the kinematic region when  $x \lesssim x_g$ , where  $x_g$  has the following form [18],

$$x_g \approx \frac{\sqrt{3}}{f_g m_N R_A^{ch}}. \quad (4.1)$$

Here, the factor  $f_g = \langle l_c \rangle / \langle l_c^G \rangle \sim 10$  [56] and  $R_A^{ch}$  is the mean value of the nuclear charge radius.

As a first step, we verified in Fig. 1 that the model calculations of  $t$ -distributions  $d\sigma^{\gamma^*p \rightarrow J/\psi p}(t, W, Q^2 \approx 0)/dt$ ,  $d\sigma^{\gamma^*p \rightarrow J/\psi p}(t, W, Q^2 = 8.9 \text{ GeV}^2)/dt$ , as well as  $t$ -integrated  $\sigma^{\gamma^*p \rightarrow \psi' p}(W, Q^2 \approx 0)$  are in good agreement with the available data on the proton target from the H1 [60] and LHCb [61] collaborations. Then we checked that our

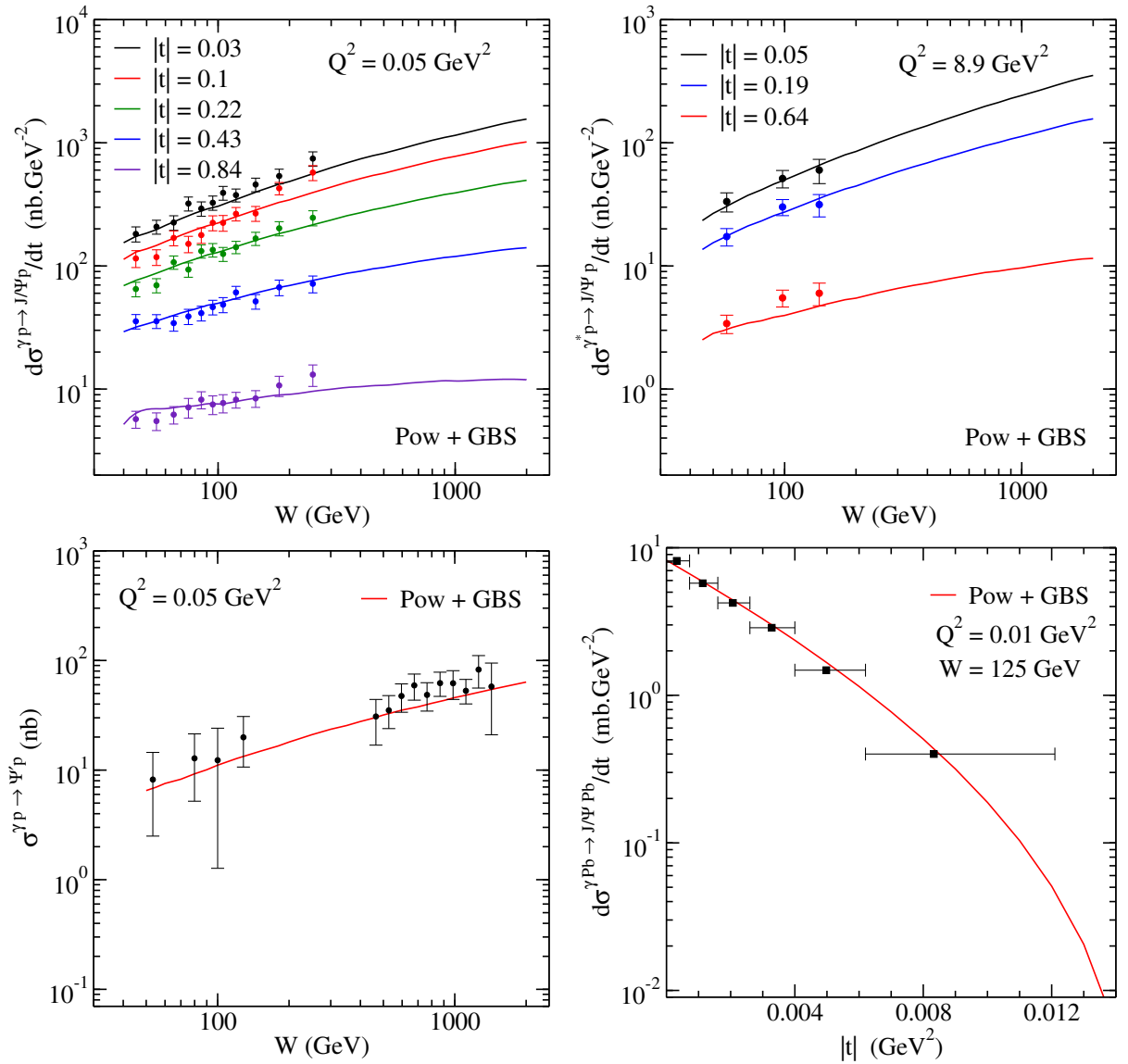


FIG. 1: Model calculations of  $d\sigma^{\gamma(\gamma^*)p \rightarrow J/\psi p}(t)/dt$  at  $Q^2 = 0.05 \text{ GeV}^2$  (upper left panel) and at  $Q^2 = 8.9 \text{ GeV}^2$  (upper right panel) as a function of photon energy  $W$  at several fixed values of  $t$  vs. data from the H1 collaboration [60]. Results for the  $t$ -integrated differential cross section in the photoproduction of  $\psi'(2S)$  are shown in the lower left panel and compared with data from the LHCb [61] collaboration. The lower right panel shows the model calculations of  $d\sigma^{\gamma P^b \rightarrow J/\psi P^b}(t)/dt$  in comparison with data from the ALICE experiment [62].

calculations describe well the first ALICE data [62] on the  $t$  dependence of coherent  $J/\psi$  photonuclear production, as demonstrated in the lower right panel of Fig. 1. In the next sections, we focus only on the heavy gold target due to the expected maximum strength of all relevant nuclear phenomena, such as the CT and (reduced) CL effects, as well as the gluon shadowing.

## B. Manifestations of CT effects

The effect of CT leads to a modification of the diffractive pattern in  $d\sigma^{\gamma^* A \rightarrow V A}/dt$  which results in a shifted positions of the diffractive minima to larger values of  $t$ , as shown in Fig. 2. Here we present model calculations in the

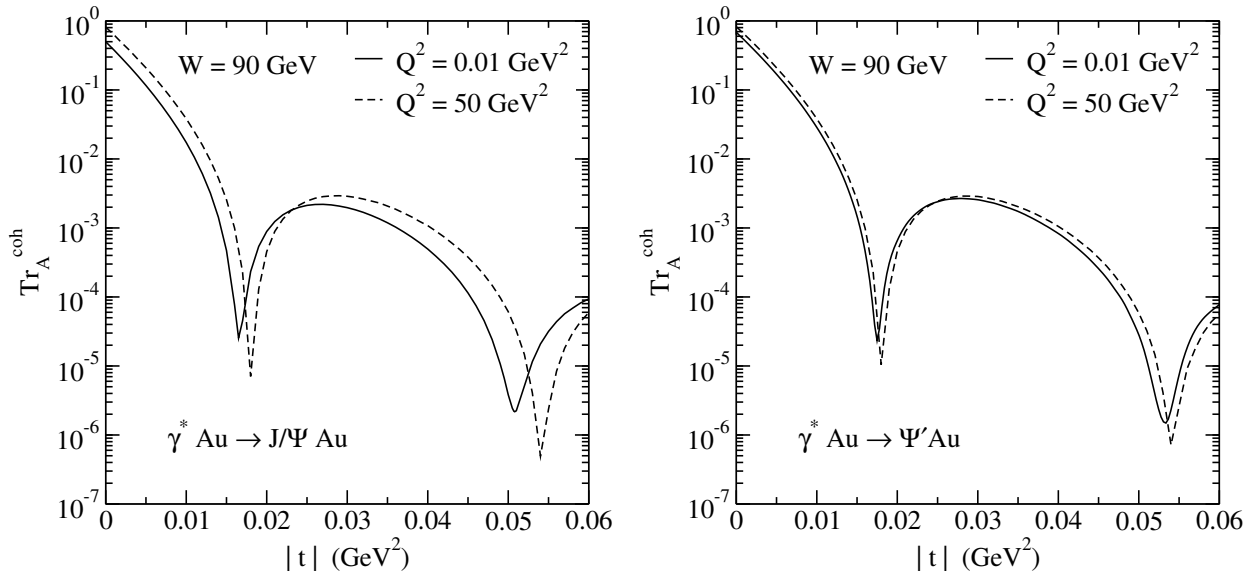


FIG. 2: The  $t$ -dependent nuclear transparency, Eq. (4.2), for the coherent electroproduction of  $J/\psi(1S)$  (left panel) and  $\psi'(2S)$  (right panel) in the limit  $l_c \gg R_A$  and at two fixed values of  $Q^2 = 0$  and  $50 \text{ GeV}^2$ .

LCL regime ( $l_c \gg R_A$ ) of the  $t$ -dependent nuclear transparency, defined as,

$$Tr_A^{coh}(t) = \frac{d\sigma^{\gamma^* A \rightarrow VA}/dt}{A^2 d\sigma^{\gamma^* N \rightarrow VN}/dt|_{t=0}} = \frac{|\mathcal{A}^{\gamma^* A \rightarrow VA}(x, Q^2, t)|^2}{A^2 |\mathcal{A}^{\gamma^* p \rightarrow Vp}(x, Q^2, t=0)|^2}, \quad (4.2)$$

at two fixed values of  $Q^2 = 0$  and  $50 \text{ GeV}^2$ . In the LCL regime given by Eqs. (3.9) and (3.10), the amplitude in the numerator of Eq. (4.2) can be expressed as,

$$\mathcal{A}^{\gamma^* A \rightarrow VA}(x, Q^2, t = -q^2) = 2 \int d^2 b_A e^{i\vec{q} \cdot \vec{b}_A} \mathcal{M}_A(\vec{b}_A). \quad (4.3)$$

To better understand the manifestation of CT effects, we can use the quadratic approximation of the dipole cross section in Eq. (3.10),  $\int d^2 b \text{Im} \mathcal{A}_{Q\bar{Q}}^N(\vec{r}, x, \alpha, \vec{b}) \approx C(x)r^2/2$ , as well as the Gaussian approximation of the product of the photon and vector meson wave functions,  $\Psi_V^*(\vec{r}, \alpha) \Psi_{\gamma^*}(\vec{r}, \alpha, Q^2) \propto \exp[-r^2/\langle r^2 \rangle]$ . Then the  $b_A$ -dependent amplitude in Eq. (4.3) reads,

$$\mathcal{M}_A(\vec{b}_A) = \pi \langle r^2 \rangle \cdot \frac{C(x) T_A(\vec{b}_A) \langle r^2 \rangle}{2 + C(x) T_A(\vec{b}_A) \langle r^2 \rangle} \quad \text{and} \quad \mathcal{A}^{\gamma^* p \rightarrow Vp}(x, Q^2, t=0) = \pi C(x) \langle r^2 \rangle^2, \quad (4.4)$$

which gives the following simplified form for the  $t$ -dependent nuclear transparency,

$$Tr_A^{coh}(t) = \frac{4}{A^2} \left| \int d^2 b_A e^{i\vec{q} \cdot \vec{b}_A} \frac{T_A(\vec{b}_A)}{2 + C(x) T_A(\vec{b}_A) \langle r^2 \rangle} \right|^2. \quad (4.5)$$

It can be seen from Eqs. (4.4) and (4.5) that the partial amplitude  $\mathcal{M}_A(\vec{b}_A)$  is suppressed with  $Q^2$  due to diminishing of the mean  $Q\bar{Q}$ -dipole size  $\langle r^2 \rangle$  and that the suppression is larger at smaller  $b_A$ -values. Consequently, the slope  $B_{\gamma^* A} = \langle b^2 \rangle / 2$  of the differential cross section  $d\sigma^{\gamma^* A \rightarrow VA}/dt$  should be reduced with  $Q^2$ , shifting the diffractive minima to larger values of  $t$ , as indeed shown in Fig. 2. However, observing experimentally such a CT signal by  $Q^2$  modification of the diffractive pattern is questionable due to a rather weak effect. Here, the coherent production of light vector mesons gives a better chance to investigate the CT effects since their manifestations are more visible compared to the heavy quarkonium production, as analyzed in Refs. [12, 15]. On the other hand, the CT effects could be recognized and measured by EIC experiments at RHIC and the LHeC as an increase in  $t$ -dependent nuclear transparency  $Tr_A^{coh}(t)$  with  $Q^2$  at small fixed values of  $t$ , as predicted in the left panel of Fig. 2 for electroproduction of  $J/\psi(1S)$ . The coherent electroproduction of  $\psi'(2S)$  gives almost negligible chance for investigation of such effects (see the right panel of Fig. 2).

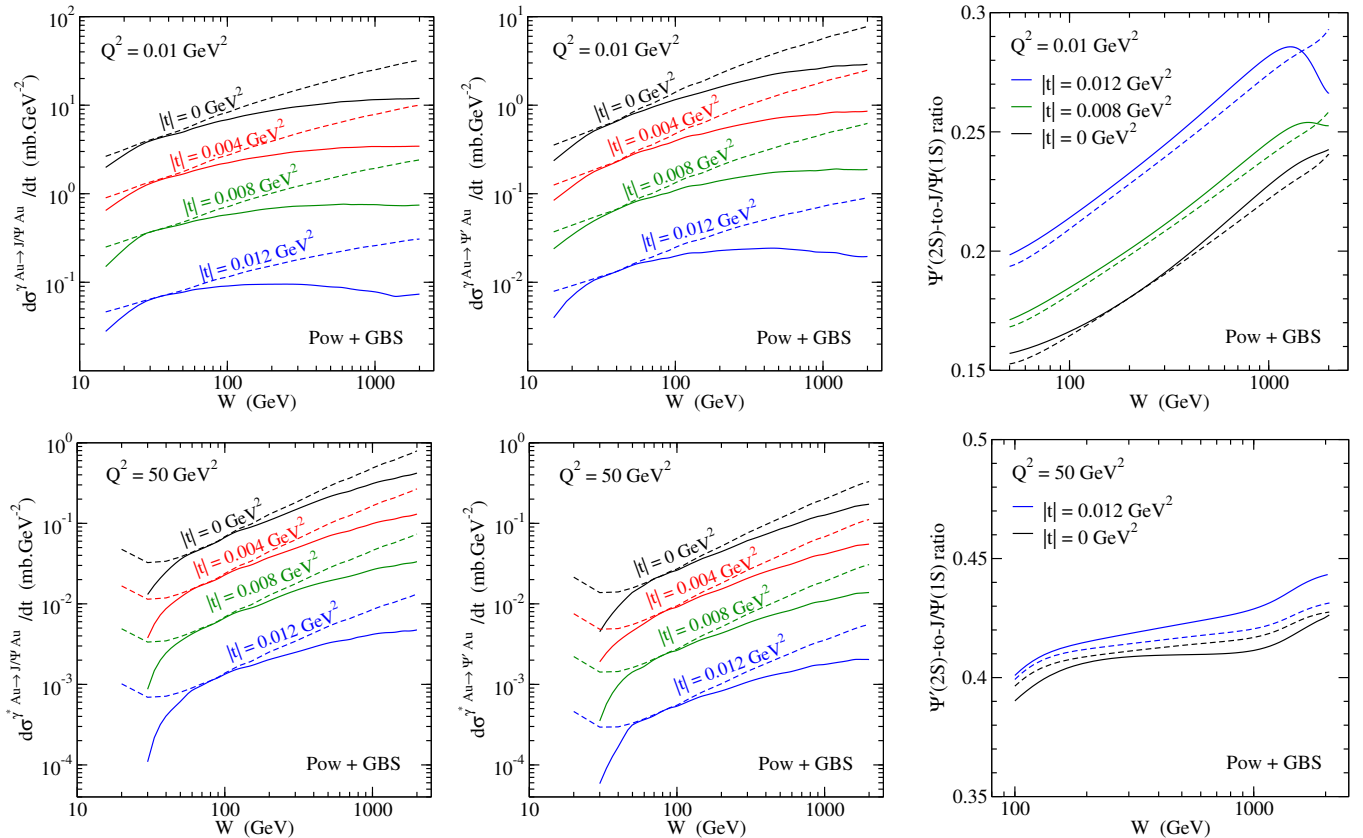


FIG. 3: Model predictions for the energy behavior of the  $t$ -dependent differential cross section  $d\sigma/dt$  for coherent photoproduction of  $J/\psi(1S)$  (upper left panel),  $\psi'(2S)$  (upper middle panel) and for the  $\psi'(2S)$ -to- $J/\psi(1S)$  ratio of  $d\sigma/dt$  (upper right panel) at several fixed values of  $t = 0, 0.004, 0.008$  and  $0.012$   $\text{GeV}^2$ . The lower panels show the electroproduction process at  $Q^2 = 50$   $\text{GeV}^2$ . In all panels the Green function formalism with gluon shadowing corrections (solid lines) is compared with the standard eikonal approximation without gluon shadowing (dashed lines).

### C. Reduced higher-twist corrections at EIC

In the EIC kinematic region at RHIC corresponding to Bjorken  $x \gtrsim x_c \approx 0.01$ , where  $x$  is given by Eq. (2.5), one should also include reduced quantum coherence effects for the lowest  $|Q\bar{Q}\rangle$  Fock state of the photon, i.e. going beyond the "frozen" eikonal approximation, Eq. (3.10). Instead of a standard approximate incorporation of such effects via the nuclear form factor depending on the longitudinal momentum transfer  $q_L = 1/l_c$  [63], we use a rigorous Green function formalism as described in the previous Sec. III. Such a formalism contains all multiple scattering terms and treats the nuclear form factor correctly. The reduced quark shadowing significantly modifies the  $t$ -dependent charmonium yields compared to the eikonal approximation at small  $W$  values, as can be seen in Fig. 3. Here we present  $d\sigma^{\gamma^* Au \rightarrow V Au}/dt$  for the coherent photoproduction of 1S and 2S charmonium states,  $V = J/\psi(1S)$  and  $\psi'(2S)$ , on the gold target and their 2S-to-1S ratio as a function of the photon energy  $W$  for several fixed values of  $t$  (upper panels). The lower panels of Fig. 3 show the analogous model predictions as the upper panels but for the coherent electroproduction process at  $Q^2 = 50$   $\text{GeV}^2$ .

Fig. 3 demonstrates that in the EIC kinematic region, the onset of reduced  $l_c$ -effects at the same photon energy is stronger in charmonium electroproduction compared to photoproduction process, in consistency with Eq. (1.1). Whereas in the photoproduction limit ( $Q^2 \approx 0$ ) such effects can be experimentally recognized only at rather small  $W \lesssim 20$   $\text{GeV}$ , i.e. at the lower limit of the kinematic region of future EIC experiments (see the upper left and middle panels of Fig. 3), charmonium electroproduction at  $Q^2 = 50$   $\text{GeV}^2$  provides a better chance for experimental investigation of reduced quark shadowing, which occurs over a wider energy range,  $W \lesssim 50$   $\text{GeV}$  (see differences between solid and dashed lines in the lower left and lower middle panels of Fig. 3).

### D. Searching for the gluon saturation at LHeC

The LHeC kinematic region provides a good basis for searching for possible manifestations of gluon saturation effects. Here the charmonium photoproduction is more suitable compared to electroproduction process due to a stronger onset of the leading-twist shadowing corrections. The corresponding factor  $R_G$  in Eq. (3.12) causes a sizable reduction of the gluon distribution function in a free nucleon at small dipole separations  $r \lesssim R_0(x, \mu^2)$  and only very slowly (logarithmically) is approaching unity as  $Q^2 \rightarrow \infty$ . The interpretation of the gluon shadowing phenomenon is reference-frame dependent. It can be treated as glue-gluon fusion in the infinite momentum frame of the nucleus. The corresponding Lorentz contraction of the nucleus keeps still a sufficiently large separations of the bound nucleons, except the gluon clouds of the nucleons that are contracted less due to their smaller momentum fraction  $x$  of the nucleon. Then gluons originating from different nucleons can overlap and interact with each other with their subsequent fusion leading to a reduction in gluon density. This corresponds to a non-linear QCD evolution incorporated into evolution equations [26, 27, 32, 33].

The leading-twist shadowing corrections in coherent charmonium photoproduction off nuclei, studied in the present paper, may represent an effective tool in searching for gluon saturation effects. Fig. 3 shows how the gluon shadowing phenomenon affects the energy behavior of the  $t$ -dependent differential cross sections (see the differences between solid and dashed lines at large photon energies) in the production of 1S and 2S charmonium states and their 2S-to-1S ratios at different fixed values of  $t$  and at  $Q^2 \approx 0$  (upper panels) and  $Q^2 = 50 \text{ GeV}^2$  (lower panels). One can see that, within the LHeC energy range of  $W \lesssim 2000 \text{ GeV}$ , a monotonic rise of  $d\sigma/dt$  with the photon energy at  $t = 0$  is gradually changed for a non-monotonic shape with a maximum that is more visible at larger  $t$  values and simultaneously shifted towards smaller values of  $W$ . This result is consistent with an increase of the gluon shadowing correction with  $t$ , since the  $R_G(x, \vec{b}_A)$  factor is scanned at smaller impact-parameter values  $b_A$  (see Fig. 1 in Ref. [6]).

The upper panels of Fig. 3 demonstrate that in the photoproduction of charmonia off gold target the  $t$ -dependent positions of maxima in  $d\sigma/dt(W)$  at  $W = W_{max}$  cover a broad photon energy range, namely  $W_{max} \sim 1500 \text{ GeV}$  at  $t = 0.004 \text{ GeV}^2$ ,  $W_{max} \sim 800 \text{ GeV}$  at  $t = 0.008 \text{ GeV}^2$  and  $W_{max} \sim 200 \text{ GeV}$  at  $t = 0.012 \text{ GeV}^2$ . This gives an opportunity for a recognition of gluon saturation effects by future experiments at the LHeC. However, finding such effects may require larger  $t$  values and, consequently, the data with higher statistics.

Here we would like to note that the  $b_A$  dependence of gluon shadowing, calculated in the present paper, is crucial for evaluation of the  $t$ -dependent differential cross sections  $d\sigma/dt$ . This is in contrast to the global data analyses providing only the  $b_A$ -integrated gluon shadowing. Note that various models for the dipole-nucleon scattering amplitude can also slightly modify the kinematic region for the onset of saturation effects when a non-monotonic scenario for the energy dependence of  $d\sigma/dt$  can be shifted to smaller or larger values of  $t$ . The coherent charmonium electroproduction off nuclei reduces substantially the chance to investigate saturation effects compared to photoproduction reaction due to weaker leading-twist corrections corresponding to a weaker onset of the non-linear QCD evolution, as seen in lower panels of Fig. 3.

The potential existence and position of the maxima in the  $W$  dependence of  $d\sigma/dt$ , as a manifestation of possible gluon saturation effects, depend on the magnitude of gluon shadowing. Its determination is related to the distance  $r_g$  of the gluon propagation from the  $Q\bar{Q}$  pair, i.e. to the size of the  $GG$  dipole. The value of  $r_g$  limits the validity of the approximation  $Q\bar{Q}G \sim GG$  used for calculation of gluon shadowing. The corresponding condition reads  $\eta^2 \gg 1/r_g^2$ , which is safely satisfied in coherent charmonium photo- and electroproduction studied in this paper. In the opposite case the  $Q\bar{Q}$  pair cannot be treated as a point-like object compared to the size of the entire  $Q\bar{Q}G$  Fock state of the photon. The single diffractive data in hadronic collisions allow to extract a magnitude of  $r_g$  as was done in Ref. [31]. Here the corresponding diffraction cross section  $\propto r^4$  exhibits a larger sensitivity to the dipole separation  $r$  compared to total cross section  $\propto r^2$ . This led to the determination of the mean  $GG$  dipole size of the order of  $r_g \sim 0.3 \text{ fm}$  [31]. Such a small gluon propagation radius represents so far the only way how to resolve the long-standing problem related to the small size of the triple-Pomeron coupling. The above value of  $r_g$  is incorporated into the LF color dipole formalism via a nonperturbative  $G$ - $G$  interaction using the path integral technique.

Note that the small value of  $r_g$  is consistent with the results of other approaches, based on the instanton liquid model [64], on the QCD sum rule analysis of the gluonic formfactor of the proton [65], as well as on the lattice calculations [66]. This indicates rather small leading-twist shadowing effects in accordance with the Next-to-Leading-Order analysis of available DIS data on nuclei [67].

We predict a stronger energy dependence for  $d\sigma^{\gamma Au \rightarrow \psi'(2S)Au}/dt$  than for the coherent photoproduction of  $J/\psi(1S)$  due to the nodal structure of the radial wave function for the 2S charmonium state (compare the upper middle and upper left panel of Fig. 3). This also leads to an increase of the  $\psi'(2S)$ -to- $J/\psi(1S)$  ratio  $R_{\psi'/J/\psi}(t)$  of  $t$ -dependent differential cross sections with the photon energy, as demonstrated in the upper right panel of Fig. 3. The node effect for the 2S charmonium state gradually fades with energy and we predict a similar scenario for a non-monotonic energy behavior of  $d\sigma/dt$  as for the 1S charmonium coherent photoproduction (compare upper left and upper middle

panels of Fig. 3 at large  $W$  values). The corresponding maxima of  $d\sigma/dt$  are shifted towards larger values of  $W$ ,  $W_{max} \sim 1300$  GeV at  $t = 0.008$  GeV<sup>2</sup> and  $W_{max} \sim 500$  GeV at  $t = 0.012$  GeV<sup>2</sup>. Since the leading-twist shadowing corrections are very similar for both the 1S and 2S charmonium states, the rise of the ratio  $R_{\psi'/J/\psi}(t)$  with energy does not differ much from that without such non-linear QCD effects, as demonstrated in right panels of Fig. 3. The non-monotonic  $W$ -dependence of  $d\sigma/dt$  for both the 1S and 2S charmonium states with different positions of maxima may generate non-monotonic energy behavior also for the  $R_{\psi'/J/\psi}(t)$ , especially at larger  $t$  values, as demonstrated in the upper right panel of Fig. 3. However, it is questionable whether such a manifestation of gluon saturation effects can be recognized experimentally at the LHeC.

At large  $Q^2 = 50$  GeV<sup>2</sup> the node effect for the  $\psi'(2S)$  state is very weak and we predict very similar scenarios for the  $W$ -dependent  $d\sigma/dt$  in coherent electronuclear production of the both charmonium states,  $J/\psi(1S)$  and  $\psi'(2S)$  (see the lower left and lower middle panel of Fig. 3). This also leads to a very weak energy dependence of the ratio  $R_{\psi'/J/\psi}(t)$  (see the lower right panel of Fig. 3). Here we present the results only for fixed  $t = 0$  and  $t = 0.012$  GeV<sup>2</sup> because the curves at all values of  $t$  lie very close to each other.

In the present work, we tried to minimize the theoretical uncertainties related to the elimination of D-wave admixture in charmonium wave functions, to the choice of realistic  $Q - \bar{Q}$  potential together with the Melosh spin effects, to the inclusion of dipole orientation with respect to the impact parameter of the collision, as well as to the proper calculations of the leading-twist shadowing corrections consistent with other models and available diffractive data. We believe that our predictions for manifestation of gluon saturation effects are realistic and can be verified by the future LHeC experiments.

### E. Pitfalls in the search for gluon saturation effects

Here we briefly mention and comment on several aspects that may affect the shape of the  $t$ -dependent and  $t$ -integrated cross sections on the proton and nuclear targets in the kinematic region of small  $x \lesssim 10^{-4} \div 10^{-5}$ . As an example we refer to the recent work [24] (see also references therein) devoted to search for gluon saturation effects. The detailed analysis of all pitfalls, which are mentioned below, will be presented elsewhere.

#### i) Shape of quarkonium wave functions

Investigation of heavy quarkonium electroproduction off protons and nuclei is a very effective tool in searching for manifestations of saturation effects, since the uncertainties in the corresponding theoretical description are reduced [45] in comparison with light vector mesons. In addition, the node effect in radially excited heavy quarkonium states gives rise to a sensitivity to the choice of the LF quarkonium wave functions. In Ref. [24], the predictions for a possible signal of gluon saturation effects in terms of the  $R_{\psi'/J/\psi}(t)$  ratio are based on the Gaussian-like wave functions related to harmonic oscillatory (HO)  $Q-\bar{Q}$  interaction potential. Moreover, the Coulomb term, first introduced in the LF HO model for the vector meson wave functions more than thirty years ago in Refs. [42, 68], has been ignored. However, a strong evidence of such Coulomb contribution may be important at small dipole separations related to electroproduction of charmonia at large  $Q^2 \gg M_{J/\psi}^2$  and especially in the photoproduction of bottomonia, which is one of the subjects of study in Ref. [24]. Moreover, the absence of the Coulomb correction can affect the node position in radial wave functions mainly for bottomonium excited states, such as  $\Upsilon'(2S)$  and  $\Upsilon''(3S)$ . Consequently, this may have a large impact on manifestations of gluon saturation effects in the analysis of the energy dependence of ratios  $R_{\Upsilon'/\Upsilon}(t)$  and  $R_{\Upsilon''/\Upsilon}(t)$ , as was done in Ref. [24].

Besides, the HO wave functions are not fully appropriate also for description of charmonium states, since they can lead, for example, to an unexpectedly strong enhancement (possible anti-shadowing effects) in the incoherent photoproduction of  $\psi'(2S)$  on nuclear targets (see e.g., Ref. [14]). Moreover, the HO model is not able to describe the data on the  $\psi'(2S)$ -to- $J/\psi(1S)$  ratio of electroproduction cross sections as a function of the photon energy and virtuality, as can be seen in Fig. 21 of Ref. [45].

Instead, several realistic potential models can be found in the literature [49, 69–72], which include also the Coulomb correction and describe the available data well, as shown in Ref. [45]. Fig. 21 in Ref. [45] also demonstrates a large deviation between predictions based on realistic and HO potential models. Such observations rule out the universal application of the HO potential model, frequently used in the literature even without the Coulomb contribution, for description of heavy quarkonium electroproduction. For this reason, the signal of gluon saturation effects, found in model predictions of Ref. [24] should be additionally verified by calculations using other models for the  $c-\bar{c}$  and  $b-\bar{b}$  potentials.

#### ii) D-wave admixture in charmonium wave functions

Another pitfall in the investigation of gluon saturation effects concerns the unjustified D-wave admixture in charmonium wave functions, related to the photon-like structure of the  $V \rightarrow Q\bar{Q}$  transition. It leads to a large 20 ÷ 30% enhancement of the  $\psi'(2S)$ -to- $J/\psi(1S)$  ratio  $R_{\psi'/J\psi}(W)$  of production cross sections, as demonstrated in Ref. [47]. Such a D-wave effect is comparable and/or even stronger than that responsible for a contribution of the non-linear term in the Balitsky-Kovchegov evolution equation [26, 27], which leads to a stronger increase of  $R_{\psi'/J\psi}(W)$  with energy  $W$ , as analyzed in Refs. [24, 73]. Thus, a significant reduction of D-wave components in quarkonium wave functions, in consistency with solutions of the Schrödinger equation with realistic  $Q\bar{Q}$  potential models in the rest frame [74–77], causes a decrease in the ratio  $R_{\psi'/J\psi}(W)$ . This may lead to a complete elimination of any signal related to gluon saturation effects.

### iii) $\vec{r}$ - $\vec{b}$ correlation

The shape of  $d\sigma^{\gamma^* p \rightarrow J/\psi(1S)p}/dt$  is closely related to  $\vec{r}$ - $\vec{b}$  correlation which should represent an indispensable feature of the  $\vec{b}$ -dependent dipole-proton partial amplitude. The corresponding form of such an amplitude should lead, after integration over the impact parameter of the collision  $\vec{b}$ , to a correct standard dipole-proton cross section of a saturated form at  $r \gg R_0(x)$  with original parameters extracted from deep-inelastic-scattering HERA data on the proton structure functions (see Sec. II). This is not the case of parametrization of  $\text{Im}A_{Q\bar{Q}}^N(\vec{r}, x_0 = 0.01, \vec{b})$  presented in Ref. [24] as the initial condition for the BK equation, denoted as the CCV model. Here, performing integration,  $2 \int d^2b \text{Im}A_{Q\bar{Q}}^N(\vec{r}, x_0, \vec{b})$ , one obtains a pathological non-monotonic behavior of the dipole cross section  $\sigma_{Q\bar{Q}}(r, x_0)$  as a function of the dipole size  $r$ , when  $\sigma_{Q\bar{Q}}(r, x_0) \rightarrow 0$  at large  $r$  in contrast with the onset of saturation. Moreover, the CCV model also disregards the dependence on the fractional momenta  $\alpha$  of  $Q$  or  $\bar{Q}$ . These facts arise the question whether such  $\vec{r}$ - $\vec{b}$  correlation has been included properly.

To clarify this, in Fig. 4 we compare the CCV model with that used in the present paper, Eq. (2.6), denoted as the KKN model. [20, 23, 28–30]. Here we present the ratio  $R_{\perp/\parallel}(b) = \text{Im}A_{Q\bar{Q}}^N(\vec{r}, \vec{b}, \Theta = \pi/2)/\text{Im}A_{Q\bar{Q}}^N(\vec{r}, \vec{b}, \Theta = 0) \equiv N(b, \Theta = \pi/2)/N(b, \Theta = 0)$  as a function of the impact parameter of a collision  $b$  at fixed values of the dipole size corresponding to the scanning radius  $r_S$  [68] in production of  $\rho^0$  (dotted lines),  $J/\psi$  (dashed lines) and  $\Upsilon$  (solid lines) mesons, where  $r_S = Y/\sqrt{M_V^2 + Q^2}$  with  $Y_\rho = 7$ ,  $Y_{J/\psi} = 6$  and  $Y_\Upsilon = 6$ .

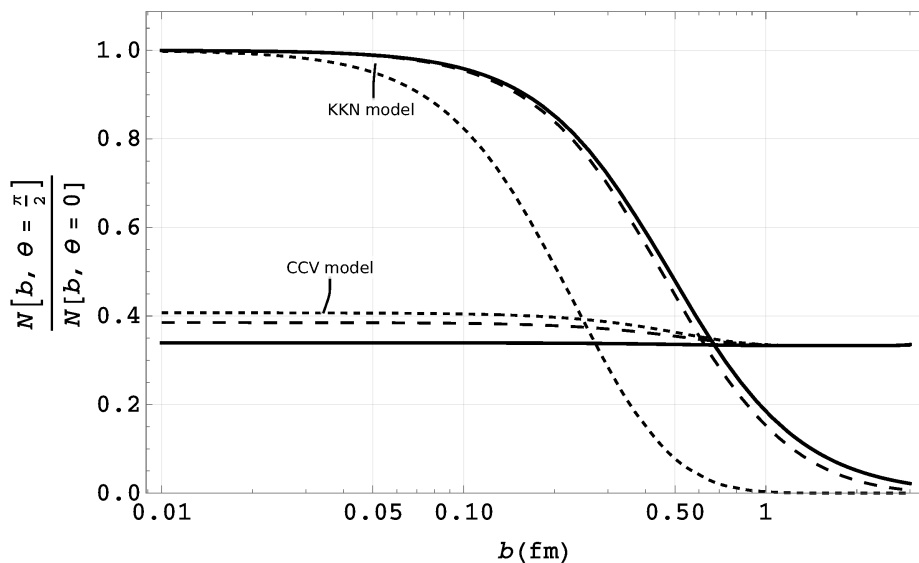


FIG. 4: (Color online) The comparison of the CCV and KKN model predictions for the ratio  $R_{\perp/\parallel}(b)$  as a function of the impact parameter of a collision  $b$ . Here the solid, dashed, and dotted lines correspond to the production of  $\Upsilon$ ,  $J/\psi$ , and  $\rho^0$  mesons, respectively.

The KKN model in Fig. 4 correctly reproduces the limits  $b \rightarrow 0$  and  $b \gg R_0(x_0)$ . In the case when  $b \rightarrow 0$ , one cannot expect any vanishing interaction, when  $\vec{r} \perp \vec{b}$ . Here the  $\vec{r}$ - $\vec{b}$  correlation becomes irrelevant and the ratio  $R_{\perp/\parallel}(b \rightarrow 0) \rightarrow 1$ . However, with increasing  $b$ , the orientation  $\vec{r} \perp \vec{b}$  gradually comes into play causing a decreasing  $R_{\perp/\parallel}(b)$ , which finally tends to zero at very large  $b$ -values, when the  $Q\bar{Q}$  dipole-nucleon interaction with  $\vec{r} \perp \vec{b}$  completely ceases compared to  $\vec{r} \parallel \vec{b}$  orientation. Fig. 4 also demonstrates a correct hierarchy in production of various

vector mesons, namely that the ratio  $R_{\perp/\parallel}(b)$  starts to decrease with  $b$  firstly for  $\rho^0$  mesons with the largest scanning radius and then for  $J/\psi$  and  $\Upsilon$  mesons. In contrast to the KKN model, the CCV model is practically insensitive to  $b$ -values, leading to an inverse hierarchy of  $R_{\perp/\parallel}(b)$  values in production of various quarkonia. For this reason, we consider this CCV model for the  $\vec{r}\text{-}\vec{b}$  correlation as incorrect.

The recent studies [24, 73] propose to investigate the  $\psi'(2S)$ -to- $J/\psi(1S)$  ratio  $R_{\psi'/J/\psi}(t, W)$  of the cross sections as a possible manifestation of gluon saturation effects. The onset of such effects should lead to a much stronger rise of  $R_{\psi'/J/\psi}(t, W)$  with the photon energy compared to the case where no saturation effects are involved. However, we have found in Refs. [20, 78] that  $\vec{r}\text{-}\vec{b}$  correlation significantly modifies the shape of  $t$ -dependent differential cross sections, reducing  $R_{\psi'/J/\psi}(t, W)$  and causing a more flat  $t$  dependence and a stronger rise with the photon energy compared to the case when vectors  $\vec{b}$  and  $\vec{r}$  are parallel. Thus, a correct incorporation of  $\vec{r}\text{-}\vec{b}$  correlation effects is unavoidable in calculations and may affect substantially the expected signal of gluon saturation. Specific detailed calculations will be presented in our forthcoming paper.

#### iv) Kernel in the BK equation

The solution of the BK evolution equation depends strongly on the Kernel, which has been adopted, e.g. in Ref. [24] in the form, which is inconsistent with the finite gluon propagation radius supported by data on gluon radiation [31, 55]. Calculations should be performed with BK Kernel corresponding to non-perturbative quark-gluon wave function [31] due to rather large mean quark-gluon separation  $r_g \sim 0.3$  fm, which is independent of  $m_Q$  and/or  $Q^2$  (up to Log corrections), but is dependent on the scale, the effective gluon mass,  $m_g \approx 0.7$  GeV. This may significantly modify the model predictions for  $d\sigma^{\gamma^*p \rightarrow J/\psi(1S)p}/dt$  compared to the results presented in Ref. [24]. Such a modification may affect conclusions about manifestations of gluon saturation effects.

#### v) Reduced shadowing effects in the BK equation for the dipole-nucleus amplitude

In description of heavy quarkonium electroproduction off nuclei, the BK equation for the eikonalized dipole-nucleus partial amplitude, Eq. (3.10), cannot be applied to nuclear targets. The reason is that all dipoles with different numbers of gluons are treated as long-lived photon fluctuations contributing to nuclear shadowing in a maximal strength. Such a result does not correspond to the fact that each additional gluon in the photon Fock state significantly reduces the corresponding coherence length, thus causing a gradual diminishing of contributions to shadowing effects from the photon components containing more and more gluons (see Sec. IV B in Ref. [6]). As a consequence, the BK equation can significantly overestimate the nuclear shadowing at large  $W$ , which may have a direct impact on the search for gluon saturation effects. The first simplified calculations in Ref. [7] show that in the LHC kinematic region the BK equation in combination with the frequently used eikonal form, Eq. (3.10), for the dipole-nucleus partial amplitude leads to an overestimation of the shadowing effects by about 20%. The modification of the BK evolution equation to include such reduced coherence effects will be presented elsewhere.

## V. SUMMARY

The transverse momentum transfer dependence of differential cross sections  $d\sigma/dt$  for the coherent electroproduction of heavy quarkonia on nuclei was studied in the framework of the dipole description based on a rigorous Green function formalism. We have analyzed a significance of the reduced effects of quantum coherence in the EIC kinematic region at RHIC, as well as leading-twist corrections at LHeC energies. The latter effect can also be treated as a manifestation of non-linear QCD effects related to gluon saturation.

In order to minimize theoretical uncertainties in our predictions, we consider the following:

- We include the correlation between impact parameter of a collision  $\vec{b}$  and the dipole orientation  $\vec{r}$ .
- We use the structure for the  $V \rightarrow Q\bar{Q}$  transition which eliminates the exaggerated weight of the D-wave component in the rest frame quarkonium wave function, in consistency with the solutions of the Schrödinger equation.
- We rely on LF wave functions of heavy quarkonia generated from a solution of the Lorentz boosted Schrödinger equation with realistic potentials together with Melosh spin rotation effects.

Each Fock component of the incoming photon, i.e.  $|\bar{Q}Q\rangle$ ,  $|\bar{Q}QG\rangle$ ,  $|\bar{Q}Q2G\rangle$ , ..., contributes independently to the heavy quarkonium electroproduction on nuclear targets in accordance with the corresponding coherence lengths. The UPC energy range at the LHC allows the eikonalization of the partial  $\vec{b}$ -dependent dipole  $Q\bar{Q}$ -proton amplitude (see Eq. (3.10)), since the coherence length for the lowest  $Q\bar{Q}$  Fock state considerably exceeds the nuclear size,  $l_c \gg R_A$ . The corresponding quark shadowing gradually diminishes with the heavy quarkonium mass and thus represents a higher-twist effect.

However, a part of the kinematic region of the prepared EIC experiments at RHIC will cover quite large  $x \gtrsim x_c \approx 0.01$ , and one eventually has to deal with reduced coherence effects, when  $l_c \lesssim R_A$ . Therefore, we apply a rigorous path integral technique for calculations of  $t$ -dependent differential cross sections and derive the corresponding formulas (see Eqs. (3.5) and (3.6)). The incorporation of the reduced  $l_c$  effects represents the main advancement of our present work. The reduced  $l_c$  effects lead to a significant decrease in the yields of  $t$ -dependent charmonium production. The corresponding predictions for  $d\sigma^{\gamma^* A \rightarrow V A}/dt$  ( $V = J/\psi(1S), \psi'(2S)$ ) can be tested by future EIC experiments at RHIC.

The high-energy part of the EIC kinematic region, when  $x \lesssim x_g$ , requires also to include shadowing corrections from the higher Fock components of the photon,  $|\bar{Q}QG\rangle, |\bar{Q}Q2G\rangle$ , etc. Such corrections are known as the gluon shadowing, which is the leading-twist effect because the transverse size of the  $Q\bar{Q}-G$  dipoles is large and nearly scale independent. They are much stronger than the higher-twist shadowing and their calculations have to rely on the path integral technique, because the dipoles  $Q\bar{Q}-G, \dots$ , cannot be treated as "frozen" even at very high energies due to a divergent  $d\alpha_g/\alpha_g$  behavior.

Coherent photoproduction of charmonia off nuclei at large LHeC energies, where the coherence length  $l_c^G \gg 2$  fm, favors to analyze the dominant role of gluon shadowing corrections allowing a subsequent study of a significance of gluon saturation effects. We predict a non-monotonic energy dependence of  $d\sigma/dt$  (see Fig. 3) that is more visible at larger  $t$  values with corresponding maxima shifted towards smaller photon energies. Such an energy behavior of  $d\sigma/dt$  can be verified by future EIC experiments at planned LHeC.

The Green function formalism also allows us to study the manifestations of color transparency effects as a modification of the shape of  $d\sigma/dt$  and/or  $Tr_A^{coh}(t)$  with  $Q^2$ . We have found that such effects lead to a shift of the diffraction minima towards larger values of  $t$  (see Fig. 2), caused by a  $Q^2$ -reduction of the slope  $B_{\gamma^* A}(Q^2)$  of the  $t$ -distributions. However, it will be difficult to detect it experimentally. The only way to detect CT effects by EIC experiments at RHIC and the LHeC is to measure an increase of  $t$ -dependent nuclear transparency with  $Q^2$  at fixed values of  $t$ , as seen in Fig. 2 for the electroproduction of  $J/\psi(1S)$ .

We briefly discussed that conclusions about the manifestations of possible gluon saturation effects should be taken with a grain of salt until the pitfalls that cause significant modification of quarkonium production rates are resolved and clarified, such as the shape of the  $Q-\bar{Q}$  interaction potential, an unjustified enhanced D-wave admixture in quarkonium wave functions, a correct model for the correlation between dipole orientation and impact parameters of a collision, the form of the realistic Kernel in the BK equation consistent with the finite gluon propagation radius, and reduced effects of quantum coherence in the BK equation. The study of radially excited heavy quarkonia at the EIC will provide a greater sensitivity to the manifestation of all these particular phenomena compared to production of 1S ground states. This can represent a very powerful tool for ruling out various phenomenological models that are seeking conclusive evidence of saturation effects.

### Acknowledgments

The work of J.N. was partially supported by the Slovak Funding Agency, Grant No. 2/0020/22. Computational resources were provided by the e-INFRA CZ project (ID:90254), supported by the Ministry of Education, Youth and Sports of the Czech Republic.

- 
- [1] C. A. Bertulani, S. R. Klein and J. Nystrand, "Physics of ultra-peripheral nuclear collisions," *Ann. Rev. Nucl. Part. Sci.* **55**, 271 (2005).
  - [2] T. H. Bauer, R. D. Spital, D. R. Yennie and F. M. Pipkin, "The Hadronic Properties of the Photon in High-Energy Interactions," *Rev. Mod. Phys.* **50**, 261 (1978) [erratum: *Rev. Mod. Phys.* **51**, 407 (1979)].
  - [3] J. Hüfner, B. Kopeliovich and J. Nemchik, "Glauber multiple scattering theory for the photoproduction of vector mesons off nuclei and the role of the coherence length," *Phys. Lett. B* **383**, 362 (1996).
  - [4] P. Agostini *et al.* [LHeC and FCC-he Study Group], "The Large Hadron–Electron Collider at the HL-LHC," *J. Phys. G* **48**, 110501 (2021).
  - [5] B. Z. Kopeliovich, M. Krelina, J. Nemchik and I. K. Potashnikova, "Ultraperipheral nuclear collisions as a source of heavy quarkonia," *Phys. Rev. D* **107**, 054005 (2023).
  - [6] B. Z. Kopeliovich, M. Krelina, J. Nemchik and I. K. Potashnikova, "Coherent photoproduction of heavy quarkonia on nuclei," *Phys. Rev. D* **105**, 054023 (2022).
  - [7] J. Nemchik and B. Z. Kopeliovich, "Nuclear Effects in Coherent Photoproduction of Heavy Quarkonia," *Acta Phys. Polon. Supp.* **16**, 7 (2023).
  - [8] M. Krelina, V. P. Goncalves and J. Cepila, "Coherent and incoherent vector meson electroproduction in the future electron-ion colliders: the hot-spot predictions," *Nucl. Phys. A* **989**, 187 (2019). doi:10.1016/j.nuclphysa.2019.06.009

- [9] A. Accardi *et al.*; “Electron Ion Collider: The Next QCD Frontier : Understanding the glue that binds us all,” *Eur. Phys. J. A* **52**, 268 (2016).
- [10] E.C. Aschenauer *et al.*; “eRHIC Design Study: An Electron-Ion Collider at BNL,” arXiv:**1409.1633** [physics.acc-ph].
- [11] E.C. Aschenauer *et al.*; “The Electron-Ion Collider: Assessing the Energy Dependence of Key Measurements,” arXiv:**1708.01527** [nucl-ex].
- [12] B. Z. Kopeliovich, J. Nemchik, A. Schafer and A. V. Tarasov, “Color transparency versus quantum coherence in electroproduction of vector mesons off nuclei,” *Phys. Rev. C* **65**, 035201 (2002).
- [13] B.Z. Kopeliovich, L.I. Lapidus and A.B. Zamolodchikov; “Dynamics of Color in Hadron Diffraction on Nuclei,” *JETP Lett.* **33**, 595 (1981) [*Pisma Zh. Eksp. Teor. Fiz.* **33**, 612 (1981)].
- [14] B.Z. Kopeliovich and B.G. Zakharov; “Quantum effects and color transparency in charmonium photoproduction on nuclei,” *Phys. Rev. D* **44**, 3466 (1991).
- [15] J. Nemchik, “Incoherent production of charmonia off nuclei as a good tool for study of color transparency,” *Phys. Rev. C* **66**, 045204 (2002).
- [16] B. Z. Kopeliovich, J. Nemchik and I. Schmidt, “Color Transparency at Low Energies: Predictions for JLAB,” *Phys. Rev. C* **76**, 015205 (2007).
- [17] J. Hüfner, Y.P. Ivanov, B.Z. Kopeliovich and A.V. Tarasov; “Photoproduction of charmonia and total charmonium proton cross-sections,” *Phys. Rev. D* **62**, 094022 (2000).
- [18] Y. Ivanov, B. Kopeliovich, A. Tarasov and J. Hüfner, “Electroproduction of charmonia off nuclei,” *Phys. Rev. C* **66**, 024903 (2002).
- [19] M. Krelina, J. Nemchik, R. Pasechnik and J. Cepila, “Spin rotation effects in diffractive electroproduction of heavy quarkonia,” *Eur. Phys. J. C* **79**, 154 (2019).
- [20] B. Z. Kopeliovich, M. Krelina and J. Nemchik, “Electroproduction of heavy quarkonia: significance of dipole orientation,” *Phys. Rev. D* **103**, 094027 (2021).
- [21] J. Nemchik and J. Óbertová, “Coherent photo- and electroproduction of charmonia on nuclear targets revisited: Green function formalism,” *Phys. Rev. D* **110**, 054015 (2024).
- [22] Y. V. Kovchegov, H. Sun and Z. Tu, “Novel cross section ratios as possible signals of saturation in ultraperipheral collisions,” *Phys. Rev. D* **109**, 094028 (2024).
- [23] B. Z. Kopeliovich, H. J. Pirner, A. H. Rezaeian and I. Schmidt, “Azimuthal anisotropy of direct photons,” *Phys. Rev. D* **77**, 034011 (2008).
- [24] J. Cepila, J. G. Contreras and M. Vaculciak, “Exclusive quarkonium photoproduction: Predictions with the Balitsky-Kovchegov equation including the full impact-parameter dependence,” *Phys. Rev. D* **111**, 056002 (2025).
- [25] H. Mäntysaari, J. Penttala, F. Salazar and B. Schenke, “Finite-size effects on small-x evolution and saturation in proton and nuclear targets,” *Phys. Rev. D* **111**, 5 (2025).
- [26] I. Balitsky, “Operator expansion for high-energy scattering,” *Nucl. Phys. B* **463**, 99 (1996).
- [27] Y. V. Kovchegov, “Small-x  $F_2$  structure function of a nucleus including multiple pomeron exchanges,” *Phys. Rev. D* **60**, 034008 (1999).
- [28] B. Z. Kopeliovich, A. H. Rezaeian and I. Schmidt, “Handedness of direct photons,” *Braz. J. Phys.* **38**, 443 (2008).
- [29] B. Z. Kopeliovich, A. H. Rezaeian and I. Schmidt, “Azimuthal Asymmetry of Prompt Photons in Nuclear Collisions,” *Nucl. Phys. A* **807**, 61 (2008).
- [30] B. Z. Kopeliovich, A. H. Rezaeian and I. Schmidt, “Azimuthal Asymmetry of pions in pp and pA collisions,” *Phys. Rev. D* **78**, 114009 (2008).
- [31] B. Z. Kopeliovich, A. Schäfer and A. V. Tarasov; “Nonperturbative effects in gluon radiation and photoproduction of quark pairs,” *Phys. Rev. D* **62**, 054022 (2000).
- [32] L.V. Gribov, E.M. Levin and M.G. Ryskin, “Singlet Structure Function at Small x: Unitarization of Gluon Ladders,” *Nucl. Phys. B* **188**, 555 (1981).
- [33] L.V. Gribov, E.M. Levin and M.G. Ryskin, “Semihard Processes in QCD,” *Phys. Rept.* **100**, 1 (1983).
- [34] J. Cepila, J. G. Contreras, M. Matas and A. Ridzikova, “Incoherent  $J/\psi$  production at large  $-t-$  identifies the onset of saturation at the LHC,” *Phys. Lett. B* **852**, 138613 (2024).
- [35] M. G. Ryskin, R. G. Roberts, A. D. Martin and E. M. Levin, “Diffractive  $J/\psi$  photoproduction as a probe of the gluon density,” *Z. Phys. C* **76**, 231 (1997).
- [36] K.J. Golec-Biernat and M. Wusthoff, “Saturation effects in deep inelastic scattering at low  $Q^2$  and its implications on diffraction,” *Phys. Rev. D* **59**, 014017 (1998).
- [37] K.J. Golec-Biernat and M. Wusthoff, “Saturation in diffractive deep inelastic scattering,” *Phys. Rev. D* **60**, 114023 (1999).
- [38] K. Golec-Biernat and S. Sapeta, “Saturation model of DIS : an update,” *JHEP* **03**, 102 (2018).
- [39] S. Chekanov *et al.* [ZEUS], “Exclusive  $\rho^0$  production in deep inelastic scattering at HERA,” *PMC Phys. A* **1**, 6 (2007).
- [40] J. Nemchik, N.N. Nikolaev, E. Predazzi, B.G. Zakharov and V.R. Zoller, “The diffraction cone for exclusive vector meson production in deep inelastic scattering” *J. Exp. Theor. Phys.* **86**, 1054 (1998).
- [41] J. B. Bronzan, G. L. Kane and U. P. Sukhatme, “Obtaining Real Parts of Scattering Amplitudes Directly from Cross-Section Data Using Derivative Analyticity Relations,” *Phys. Lett. B* **49**, 272 (1974).
- [42] J. Nemchik, N. N. Nikolaev, E. Predazzi and B. G. Zakharov, “Color dipole phenomenology of diffractive electroproduction of light vector mesons at HERA,” *Z. Phys. C* **75**, 71 (1997).
- [43] J. R. Forshaw, R. Sandapen and G. Shaw, “Color dipoles and  $\rho$ ,  $\phi$  electroproduction,” *Phys. Rev. D* **69**, 094013 (2004).
- [44] A. G. Shuvaev, K. J. Golec-Biernat, A. D. Martin and M. G. Ryskin, “Off diagonal distributions fixed by diagonal partons

- at small  $x$  and  $x_i$ ,” *Phys. Rev. D* **60**, 014015 (1999).
- [45] J. Cepila, J. Nemchik, M. Krelina and R. Pasechnik, “Theoretical uncertainties in exclusive electroproduction of S-wave heavy quarkonia,” *Eur. Phys. J. C* **79**, 495 (2019).
- [46] M. Krelina, J. Nemchik and R. Pasechnik, “D-wave effects in diffractive electroproduction of heavy quarkonia from the photon-like  $V \rightarrow Q\bar{Q}$  transition,” *Eur. Phys. J. C* **80**, 92 (2020).
- [47] M. Krelina and J. Nemchik, “D-wave effects in heavy quarkonium production in ultraperipheral nuclear collisions,” *Phys. Rev. D* **102**, 114033 (2020).
- [48] B. Z. Kopeliovich, E. Levin, I. Schmidt and M. Siddikov, “Lorentz-boosted description of a heavy quarkonium,” *Phys. Rev. D* **92**, 034023 (2015).
- [49] N. Barik and S.N. Jena, “Fine - Hyperfine Splittings Of Quarkonium Levels In An Effective Power Law Potential,” *Phys. Lett. B* **97**, 265 (1980).
- [50] M. V. Terentev, “On the Structure of Wave Functions of Mesons as Bound States of Relativistic Quarks,” *Sov. J. Nucl. Phys.* **24**, 106 (1976) [*Yad. Fiz.* **24**, 207 (1976)].
- [51] H.J. Melosh, “Quarks: Currents and constituents,” *Phys. Rev. D* **9**, 1095 (1974).
- [52] T. Lappi, H. Mäntysaari and J. Penttala, “Relativistic corrections to the vector meson light FRONT wave function,” *Phys. Rev. D* **102**, 054020 (2020).
- [53] H.De Vries, C.W.De Jager and C.De Vries, “Nuclear charge and magnetization density distribution parameters from elastic electron scattering,” *Atom. Data Nucl. Data Tabl.* **36**, 495 (1987).
- [54] Y. Ivanov, B. Kopeliovich and I. Schmidt, “Vector meson production in ultra-peripheral collisions at LHC,” arXiv:0706.1532 [hep-ph].
- [55] B. Z. Kopeliovich, I. K. Potashnikova, B. Povh and I. Schmidt, “Evidences for two scales in hadrons,” *Phys. Rev. D* **76**, 094020 (2007).
- [56] B. Z. Kopeliovich, J. Raufeisen and A. V. Tarasov, “Nuclear shadowing and coherence length for longitudinal and transverse photons,” *Phys. Rev. C* **62**, 035204 (2000).
- [57] B. Kopeliovich, A. Tarasov and J. Hufner, “Coherence phenomena in charmonium production off nuclei at the energies of RHIC and LHC,” *Nucl. Phys. A* **696**, 669 (2001).
- [58] B. Kopeliovich, J. Nemchik, I. Potashnikova and I. Schmidt, “Gluon Shadowing in DIS off Nuclei,” *J. Phys. G* **35**, 115010 (2008).
- [59] M. Krelina and J. Nemchik, “Nuclear shadowing in DIS at electron-ion colliders,” *Eur. Phys. J. Plus* **135**, 444 (2020).
- [60] A. Aktas *et al.* [H1], “Elastic  $J/\psi$  production at HERA,” *Eur. Phys. J. C* **46**, 585 (2006).
- [61] R. Aaij *et al.* [LHCb], “Central exclusive production of  $J/\psi$  and  $\psi(2S)$  mesons in  $pp$  collisions at  $\sqrt{s} = 13$  TeV,” *JHEP* **10**, 167 (2018).
- [62] S. Acharya *et al.* [ALICE], “First measurement of the  $t$ -dependence of coherent  $J/\psi$  photonuclear production,” *Phys. Lett. B* **817**, 136280 (2021).
- [63] B. Z. Kopeliovich, J. Nemchik, N. N. Nikolaev and B. G. Zakharov, “Novel color transparency effect: Scanning the wave function of vector mesons,” *Phys. Lett. B* **309**, 179 (1993).
- [64] T. Schäfer and E. V. Shuryak, “Instantons in QCD,” *Rev. Mod. Phys.* **70**, 323 (1998).
- [65] V. M. Braun, P. Gornicki, L. Mankiewicz and A. Schafer, “Gluon form-factor of the proton from QCD sum rules,” *Phys. Lett. B* **302**, 291 (1993).
- [66] M. D’Elia, A. Di Giacomo and E. Meggiolaro, “Field strength correlators in full QCD,” *Phys. Lett. B* **408**, 315 (1997).
- [67] D. de Florian, R. Sassot, P. Zurita and M. Stratmann, “Global Analysis of Nuclear Parton Distributions,” *Phys. Rev. D* **85**, 074028 (2012).
- [68] J. Nemchik, N. N. Nikolaev and B. G. Zakharov, “Scanning the BFKL pomeron in elastic production of vector mesons at HERA,” *Phys. Lett. B* **341**, 228 (1994).
- [69] E. Eichten, K. Gottfried, T. Kinoshita, K.D. Lane and T.M. Yan; “Charmonium: Comparison with Experiment,” *Phys. Rev. D* **21**, 203 (1980).
- [70] E. Eichten, K. Gottfried, T. Kinoshita, K.D. Lane and T.M. Yan; “Charmonium: The Model,” *Phys. Rev. D* **17**, 3090 (1978); Erratum: [*Phys. Rev. D* **21**, 313 (1980)].
- [71] C. Quigg and J.L. Rosner; “Quarkonium Level Spacings,” *Phys. Lett. B* **71**, 153 (1977).
- [72] W. Buchmuller and S.H.H. Tye, “Quarkonia and Quantum Chromodynamics,” *Phys. Rev. D* **24**, 132 (1981).
- [73] M. A. Peredo and M. Hentschinski, “Ratio of  $J/\psi$  and  $\psi(2s)$  exclusive photoproduction cross sections as an indicator for the presence of nonlinear QCD evolution,” *Phys. Rev. D* **109**, 014032 (2024).
- [74] I. Haysak, Y. Fekete, V. Morokhovych, S. Chalupka and M. Salak, “Spin effects in two quark system and mixed states,” *Czech. J. Phys.* **55**, 541 (2005).
- [75] H. F. Fu and L. Jiang, “Coupled-channel-induced  $S-D$  mixing of Charmonia and testing possible assignments for  $Y(4260)$  and  $Y(4360)$ ,” *Eur. Phys. J. C* **79**, 460 (2019).
- [76] C. Chang and G. Wang, “Spectrum for Heavy Quarkonia and Mixture of the Relevant Wave Functions within the Framework of Bethe-Salpeter Equation,” *Sci. China Phys. Mech. Astron.* **53**, 2005 (2010).
- [77] L. Cao, Y. C. Yang and H. Chen, “Charmonium states in QCD-inspired quark potential model using Gaussian expansion method,” *Few Body Syst.* **53**, 327 (2012).
- [78] M. Krelina and J. Nemchik, “Momentum transfer dependence of heavy quarkonium electroproduction,” *SciPost Phys. Proc.* **8**, 114 (2022).